J Eng Math (2009) 63:95–119
DOI 10.1007/s10665-008-9234-2

Cylindrical bending vibration of functionally graded piezoelectric shells using the method of perturbation

Chih-Ping Wu · Yi-Hwa Tsai

Received: 3 November 2007 / Accepted: 16 May 2008 / Published online: 11 June 2008

Abstract Based on the three-dimensional (3D) piezoelectricity, two asymptotic formulations for the cylindrical bending vibration of simply supported, functionally graded (FG) piezoelectric cylindrical shells with open-circuit and closed-circuit surface conditions are presented. The normal electric displacement and electric potential are prescribed to be zero on the lateral surfaces. In the present asymptotic formulations the material properties are regarded to be heterogeneous through the thickness coordinate. Afterwards, they are further specified to be constant in single-layer shells, to be layerwise constant in multilayered shells and to obey an identical exponent-law distribution in FG shells. The method of multiple time scales is used to eliminate the secular terms arising from the regular asymptotic expansion. The orthonormality and solvability conditions for various orders are derived. The recursive property among the motion equations of various order problems is shown. The present asymptotic formulations are applied to several illustrative examples. The accuracy and the rate of convergence of the present asymptotic solutions are evaluated. The coupled electro–elastic effect and the influence of the material-property gradient index on the free-vibration behavior of FG piezoelectric shells are studied.

Keywords 3D solutions · Analytical modeling · Piezoelectric shells · Smart materials · Vibration

1 Introduction

In recent years, a new class of functionally graded (FG) piezoelectric materials has being widely used as smart structures in engineering applications. Since these materials possess natural coupling effects between the electric and elastic fields, they have successfully been used to form self-monitoring and self-controlling devices. The subjects on the exact three-dimensional (3D) analysis of FG piezoelectric structures have therefore attracted the researchers' attention.

The class of multilayered piezoelectric plates and shells can be regarded as a special case of FG piezoelectric plates and shells where the material properties of these structures are layer-wise constant distributions through the thickness coordinate. Based on a discrete-layer theory, Hussein and Heyliger [1] presented exact solutions for the free-vibration behavior of laminated piezoelectric cylinders with both open-circuit and closed-circuit surface conditions. Natural frequencies and their corresponding modal field variables through the thickness coordinate for

C.-P. Wu (✉) · Y.-H. Tsai
Department of Civil Engineering, National Cheng Kung University, Tainan, Taiwan, ROC
e-mail: cpwu@mail.ncku.edu.tw

various piezoelectric laminates were studied. The previous discrete-layer theory has also been used to investigate the axisymmetric free vibration of homogeneous and laminated piezoelectric cylinders by Kharouf and Heyliger [2] as well as the free vibration of laminated circular piezoelectric plates and disks by Heyliger and Ramirez [3]. Shu [4] presented an accurate theory for the cylindrical bending vibration of laminated piezoelectric plates. Heyliger and Brooks [5, 6] studied exact solutions for the cylindrical bending static and dynamic behaviors of multilayered piezoelectric plates using a similar approach as that of Pagano [7]. Vel et al. [8] analyzed the cylindrical bending vibration of multilayered plates with embedded or surface-mounted piezoelectric patches. Vel and Batra [9] presented exact solutions for the 3D deformations of simply supported sandwich plates with embedded piezoelectric shear actuators. Based on the state space formalism, Lü et al. [10] studied the cylindrical bending vibration of angle-ply laminates using the propagator (or transfer) matrix method. Effects of variation of ply angle on the vibration properties of laminates have been investigated. Jin and Batra [11] developed a finite-element code using eight-node isoparametric elements for the static and free-vibration analyses of multilayered piezoelectric plates. Effects of electro-mechanical coupling and open-circuit versus closed-circuit surface conditions on deformations and natural frequencies have been reported. Comprehensive reviews of theoretical analyses and numerical modeling for piezoelectric laminates have been made by Tang et al. [12], Saravanos and Heyliger [13], Gopinathan et al. [14] and Chee et al. [15].

The articles dealing with the exact 3D analysis of FG piezoelectric plates and shells are not many in comparison with those of multilayered piezoelectric plates and shells. Ramirez et al. [16] presented approximate 3D solution for the static analysis of FG elastic anisotropic plates using a discrete-layer approach. Chen and Ding [17] and Wu and Liu [18] studied the free vibration and static responses of a FG piezoelectric rectangular plate using the state space method, respectively. In their analysis, a successive approximation method firstly proposed by Soldatos and Hadjigeorgiou [19] was adopted for dividing the FG plate into certain layers with constant material coefficients. Thus, the state equations with variable coefficients can be approximately reduced to ones with constant coefficients in each layer. This discretization scheme on the material properties makes the state space method feasible for the 3D analysis of FG piezoelectric plates. Using the successive-approximation method, Shuvalov and Soldatos [20] presented the 3D static and dynamic analysis of radially inhomogeneous tubes with arbitrary cylindrical anisotropy. In [20], the successive approximation method introduced in [19] has also been demonstrated to be practically an exact method in the sense that it can approximate the exact solution of relevant problems to any desired accuracy. A sextic formalism was developed for 3D elastodynamics of cylindrically anisotropic radially inhomogeneous materials by Shuvalov [21]. Vel and Batra [22] presented 3D exact solutions for the free and forced vibrations of simply supported, FG rectangular plates using the power-series method where the material properties are estimated by either Mori–Tanaka [23] or self-consistent schemes [24]. Zhong and Yu [25] presented 3D solutions of the free and forced vibrations of a simply supported, FG piezoelectric rectangular plate with open-circuit, closed-circuit and two additional mixed surface conditions using the state space method.

An alternative analytical approach, namely the asymptotic approach apart from the aforementioned methods of state space and power series, has been proposed and successfully applied to obtain exact solutions of laminated composite plates by Wang and Tarn [26] and Tarn and Wang [27, 28] and of laminated composite shells by Wu and his colleagues [29–32]. The asymptotic approach has also been extensively applied for the analysis of laminated piezoelectric plates by Cheng and Batra [33, 34] and of laminated piezoelectric shells by Wu and his colleagues [35, 36]. Since these asymptotic formulations may account for arbitrary variations of material properties through the thickness coordinate without using a discretization scheme for FG structures, we aim at developing two different asymptotic formulations for cylindrical bending vibration of FG piezoelectric cylindrical shells with open-circuit and closed-circuit surface conditions, respectively. Asymptotic analysis for dynamic response of inhomogeneous plates and shells is not just a matter of applying a standard perturbation method. This will lead not only to equations that are too cumbersome to be useful but also nonuniform expansions containing secular terms. Hence, in the present paper, the method of multiple time scales developed by Nayfeh [37] and Nayfeh and Mook [38] has been used to eliminate the secular terms arising from the regular asymptotic expansions. These present asymptotic formulations have been applied for several cylindrical bending vibration problems of multilayered and FG piezoelectric plates and shells in illustrative examples.

2 Basic equations of piezoelectricity

We consider a simply supported, FG orthotropic piezoelectric cylindrical shell with a very large length as compared to the other two dimensions. The configuration of a typical cross-section of the shell is shown in Fig. 1. A cylindrical coordinate system with variables x, θ, r is used and located on the middle surface of the shell; $2h$ and R stand for the total thickness and the curvature radii to the middle surface of the shell, respectively; θ_α denotes the angle between two edges in the circumferential direction; a_θ is the mid-surface dimension of the shell and $a_\theta = R\theta_\alpha$. The radial coordinate r is also represented as $r = R + \zeta$ where ζ is the thickness coordinate measured from the middle surface of the shell.

The constitutive equations of piezoelectric material are given by

$$\sigma_i = c_{ij}\varepsilon_j - e_{ki}E_k, \quad D_l = e_{lj}\varepsilon_j + \eta_{lk}E_k, \tag{2.1, 2.2}$$

where σ_i, ε_j $(i, j = 1\text{–}6)$ denote the contracted notation for the stress and strain components, respectively. Further D_l and E_k $(l, k = 1\text{–}3)$ denote the components of the electric displacement and electric field, respectively; c_{ij}, e_{ij} $(i, j = 1\text{–}6)$ and $\eta_{lk}(l, k = 1\text{–}3)$ are the elastic, piezoelectric and dielectric coefficients, respectively, relative to the geometrical axes of the cylindrical shell. The material properties are considered as heterogeneous through the thickness (i.e., $c_{ij}(\zeta)$, $e_{lj}(\zeta)$ and $\eta_{lk}(\zeta)$). For an orthotropic solid, the previous material coefficients are given by

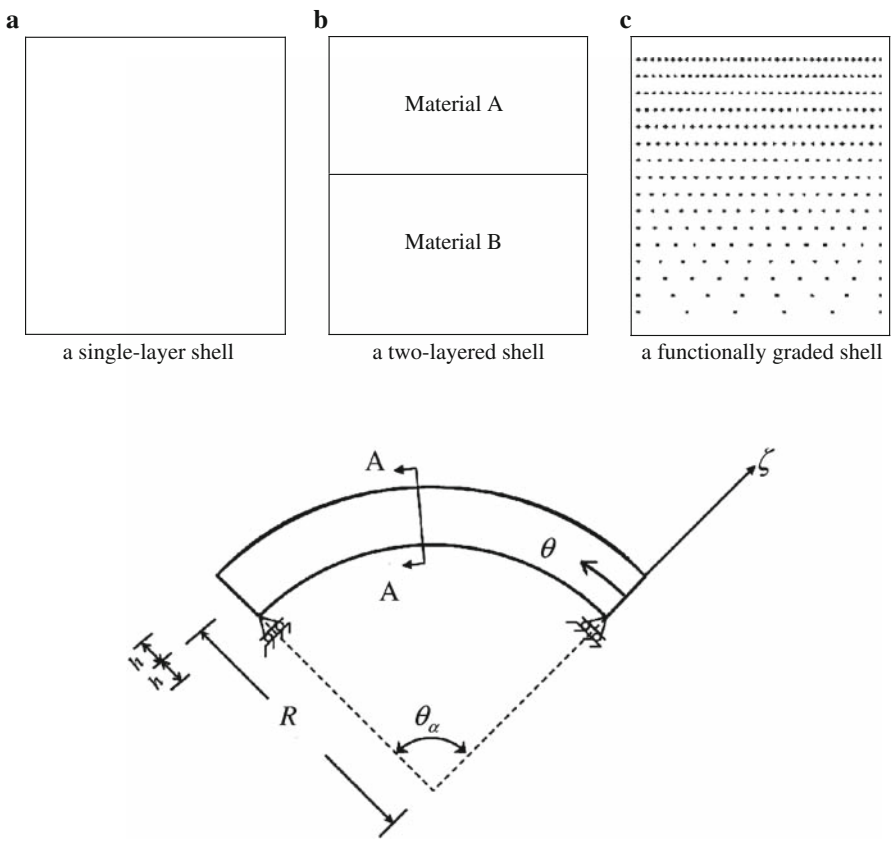

Fig. 1 The geometry and coordinates of a typical cross-section of a cylindrical strip

$$\mathbf{c}=\begin{bmatrix} c_{11} & c_{12} & c_{13} & 0 & 0 & 0 \\ c_{12} & c_{22} & c_{23} & 0 & 0 & 0 \\ c_{13} & c_{23} & c_{33} & 0 & 0 & 0 \\ 0 & 0 & 0 & c_{44} & 0 & 0 \\ 0 & 0 & 0 & 0 & c_{55} & 0 \\ 0 & 0 & 0 & 0 & 0 & c_{66} \end{bmatrix}, \quad \mathbf{e}=\begin{bmatrix} 0 & 0 & e_{31} \\ 0 & 0 & e_{32} \\ 0 & 0 & e_{33} \\ 0 & e_{24} & 0 \\ e_{15} & 0 & 0 \\ 0 & 0 & 0 \end{bmatrix}, \quad \boldsymbol{\eta}=\begin{bmatrix} \eta_{11} & 0 & 0 \\ 0 & \eta_{22} & 0 \\ 0 & 0 & \eta_{33} \end{bmatrix}.$$

For cylindrical bending problems, all the field variables are functions of the circumferential and thickness coordinates only, not of the axial coordinate. Hence, all the relative derivatives of the field variables with respect to the axial coordinate are identical to zero in the present formulation.

The strain–displacement relationships are given by

$$\varepsilon_x = 0, \quad \varepsilon_\theta = \frac{1}{r}u_{\theta,\theta} + \frac{1}{r}u_r, \quad \varepsilon_r = u_{r,r}, \tag{2.3–2.5}$$

$$\gamma_{\theta r} = u_{\theta,r} - \frac{1}{r}u_\theta + \frac{1}{r}u_{r,\theta}, \quad \gamma_{xr} = u_{x,r}, \quad \gamma_{x\theta} = \frac{1}{r}u_{x,\theta}, \tag{2.6–2.8}$$

in which u_x, u_θ and u_r are the displacement components.

The stress equations of motion in the cylindrical coordinates are given by

$$\tau_{x\theta,\theta} + \tau_{xr} + r\tau_{xr,r} = \rho r u_{x,tt}, \quad \sigma_{\theta,\theta} + r\tau_{\theta r,r} + 2\tau_{\theta r} = \rho r u_{\theta,tt}, \quad \tau_{\theta r,\theta} + r\sigma_{r,r} + \sigma_r - \sigma_\theta = \rho r u_{r,tt}, \tag{2.9–2.11}$$

where ρ denotes the mass density of the shell; t is the time variable. The charge equation of the FG piezoelectric material without electric charge density is

$$\nabla \cdot \mathbf{D} = 0, \tag{2.12}$$

where ∇ stands for the nabla operator. The relationship between the electric field and electric potential is expressed by

$$\mathbf{E} = -\nabla\Phi, \tag{2.13}$$

where Φ is the electric potential.

The boundary conditions of the problem are specified as follows:
on the lateral surfaces, the traction stresses and normal electric displacement (or electric potential) are prescribed:

$$\lfloor \tau_{xr} \quad \tau_{\theta r} \quad \sigma_r \quad D_r \rfloor = [0 \quad 0 \quad 0 \quad 0] \quad \text{on} \quad r = R \pm h \quad \text{(open-circuit conditions);} \tag{2.14a}$$

$$\lfloor \tau_{xr} \quad \tau_{\theta r} \quad \sigma_r \quad \Phi \rfloor = [0 \quad 0 \quad 0 \quad 0] \quad \text{on} \quad r = R \pm h \quad \text{(closed-circuit conditions).} \tag{2.14b}$$

The edge boundary conditions of the shell are considered as fully simple supports and suitably grounded. They are given by

$$\sigma_\theta = u_x = u_r = \Phi = 0, \quad \text{at} \quad \theta = 0 \quad \text{and} \quad \theta = \theta_\alpha. \tag{2.15}$$

3 Nondimensionalization

A set of dimensionless coordinates and elastic-field variables is defined as

$$\begin{aligned} &x_1 = x/R \in, \quad x_2 = \theta/\in, \quad x_3 = \zeta/h \quad \text{and} \quad r = R + \zeta; \\ &u_1 = u_x/R \in, \quad u_2 = u_\theta/R \in, \quad u_3 = u_r/R; \\ &\sigma_1 = \sigma_x/Q, \quad \sigma_2 = \sigma_\theta/Q, \quad \tau_{12} = \tau_{x\theta}/Q; \\ &\tau_{13} = \tau_{xr}/Q \in, \quad \tau_{23} = \tau_{\theta r}/Q \in, \quad \sigma_3 = \sigma_r/Q \in^2; \end{aligned} \tag{3.1a–d}$$

where $\in^2 = h/R$; Q denotes a reference elastic modulus.

Two different sets of dimensionless electric field variables are defined as

$$D_1 = D_x/\epsilon^{(j-1)}e, \quad D_2 = D_\theta/\epsilon^{(j-1)}e, \quad D_3 = D_r/e, \quad \phi = \Phi e/\epsilon^j RQ, \tag{3.2a–d}$$

where e denotes a reference piezoelectric modulus. In the present formulations, the superscript j is taken as zero which corresponds to open-circuit conditions where the normal electric displacement and transverse stresses are zero on the lateral surfaces; $j = 2$ corresponds to the closed-circuit conditions where the electric potential and transverse stresses are zero on the lateral surfaces.

The dimensionless multiple time scales are defined by

$$t_k = \frac{\epsilon^{2k}}{R}\sqrt{\frac{Q}{\rho_0}}t \quad (k = 0, 1, 2, \text{etc.}), \tag{3.3}$$

where ρ_0 denotes a reference mass density.

To simplify the manipulation of the whole mathematical system, we select transverse stresses $(\tau_{xr}, \tau_{\theta r}, \sigma_r)$, elastic displacements (u_x, u_θ, u_r), normal electric displacement (D_r) and electric potential (Φ) as primary field variables. The other variables are secondary field variables and can be expressed in terms of primary field variables.

By eliminating the secondary field variables from (2.1)–(2.13), and then introducing the set of dimensionless coordinates and variables (3.1)–(3.3) in the resulting equations, we can rewrite the basic equations as follows:

$$u_{3,3} = -\epsilon^2\,\bar{a}_2 u_{2,2} - \epsilon^2\,\bar{a}_2 u_3 + \epsilon^4\,\tilde{\eta}\sigma_3 + \epsilon^2\,\tilde{e}D_3, \quad u_{1,3} = \epsilon^2\tilde{S}_{55}\tau_{13}, \tag{3.4, 3.5}$$

$$u_{2,3} = -u_{3,2} + \epsilon^2\,(1 - x_3\partial_3)u_2 + \epsilon^2\,\tilde{S}_{44}\tau_{23} + \epsilon^4\,(x_3\tilde{S}_{44})\tau_{23} - \epsilon^j\,(\tilde{S}_{44}\tilde{e}_{24})\phi_{,2}, \tag{3.6}$$

$$D_{3,3} = -\epsilon^j\,D_{2,2} - \epsilon^2\,(1 + x_3\partial_3)D_3, \tag{3.7}$$

$$\tau_{13,3} = -\bar{Q}_{66}u_{1,22} - \epsilon^2\,(1 + x_3\partial_3)\tau_{13} + \rho_1\left[\frac{\partial^2}{\partial t_0^2} + 2\,\epsilon^2\,\frac{\partial^2}{\partial t_0\partial t_1} + \epsilon^4\left(2\frac{\partial^2}{\partial t_0\partial t_2} + \frac{\partial^2}{\partial t_1^2}\right) + \cdots\right]u_1, \tag{3.8}$$

$$\begin{aligned}\tau_{23,3} = {} & -\bar{Q}_{22}u_{2,22} - \bar{Q}_{22}u_{3,2} - \epsilon^2\,(2 + x_3\partial_3)\tau_{23} - \epsilon^2\,\tilde{a}_2\sigma_{3,2} - \tilde{b}_2 D_{3,2} \\ & + \rho_1\left[\frac{\partial^2}{\partial t_0^2} + 2\,\epsilon^2\,\frac{\partial^2}{\partial t_0\partial t_1} + \epsilon^4\left(2\frac{\partial^2}{\partial t_0\partial t_2} + \frac{\partial^2}{\partial t_1^2}\right) + \cdots\right]u_2,\end{aligned} \tag{3.9}$$

$$\begin{aligned}\sigma_{3,3} = {} & \bar{Q}_{22}u_{2,2} + \bar{Q}_{22}u_3 - \tau_{23,2} - \epsilon^2\,(-\tilde{a}_2 + 1 + x_3\partial_3)\sigma_3 + \tilde{b}_2 D_3 \\ & + \rho_2\left[\frac{\partial^2}{\partial t_0^2} + 2\,\epsilon^2\,\frac{\partial^2}{\partial t_0\partial t_1} + \epsilon^4\left(2\frac{\partial^2}{\partial t_0\partial t_2} + \frac{\partial^2}{\partial t_1^2}\right) + \cdots\right]u_3,\end{aligned} \tag{3.10}$$

$$\phi_{,3} = -\epsilon^{(2-j)}\,\bar{b}_2 u_{2,2} - \epsilon^{(2-j)}\,\bar{b}_2 u_3 + \epsilon^{(4-j)}\,\tilde{e}\sigma_3 - \epsilon^{(2-j)}\,\tilde{c}D_3, \tag{3.11}$$

where

$$[\hat{a}_i \quad \tilde{a}_i \quad \bar{a}_i]^T = \left(\frac{e_{33}e_{3i} + \eta_{33}c_{i3}}{e_{33}^2 + \eta_{33}c_{33}}\right)[\gamma_\theta \quad 1 \quad 1/\gamma_\theta]^T, \quad \gamma_\theta = 1 + \epsilon^2\,x_3,$$

$$[\hat{b}_i \quad \tilde{b}_i \quad \bar{b}_i]^T = \left(\frac{e_{33}c_{i3} - c_{33}e_{3i}}{e_{33}^2 + \eta_{33}c_{33}}\right)\left(\frac{e}{Q}\right)[\gamma_\theta \quad 1 \quad 1/\gamma_\theta]^T, \quad \tilde{S}_{55} = \frac{Q}{c_{55}}, \quad \tilde{S}_{44} = \frac{Q}{c_{44}},$$

$$\tilde{e}_{ij} = \frac{e_{ij}}{e}, \quad \tilde{\eta} = \frac{\eta_{33}Q}{e_{33}^2 + \eta_{33}c_{33}}, \quad \tilde{e} = \frac{e_{33}e}{e_{33}^2 + \eta_{33}c_{33}}, \quad \tilde{c} = \frac{c_{33}e^2}{(e_{33}^2 + \eta_{33}c_{33})}Q,$$

$$[\hat{Q}_{ij} \quad \tilde{Q}_{ij} \quad \bar{Q}_{ij}]^T = (Q_{ij}/Q)[\gamma_\theta \quad 1 \quad 1/\gamma_\theta]^T, \quad Q_{ij} = c_{ij} - \tilde{a}_j c_{i3} - \left(\tilde{b}_j Q/e\right)e_{3i},$$

$$\rho_1 = \rho h\gamma_\theta/\rho_0 R, \quad \rho_2 = \rho\gamma_\theta/\rho_0.$$

The secondary field variables, such as in-surface stresses and electric displacements, can be expressed in terms of the primary variables as follows:

$$\sigma_1 = \bar{Q}_{12}u_{2,2} + \bar{Q}_{12}u_3 + \in^2 \tilde{a}_1\sigma_3 + \tilde{b}_1 D_3, \quad \sigma_2 = \bar{Q}_{22}u_{2,2} + \bar{Q}_{22}u_3 + \in^2 \tilde{a}_2\sigma_3 + \tilde{b}_2 D_3, \tag{3.12, 3.13}$$

$$\tau_{12} = \bar{Q}_{66}u_{1,2}, \quad D_1 = \in^{(2-j)} \tilde{s}_{55}\tilde{e}_{15}\tau_{13}, \quad D_2 = \in^{(2-j)} \tilde{s}_{44}\tilde{e}_{24}\tau_{23} - \left[\left(\tilde{s}_{44}\tilde{e}_{24}^2 + \frac{\eta_{22}Q}{e^2}\right) \Big/ \gamma_\theta\right]\phi_{,2}. \tag{3.14–3.16}$$

In dimensionless form the boundary conditions of the problem are specified as follows:
On the lateral surface the transverse load and normal electric displacement (or electric potential) are prescribed,

$$\begin{bmatrix}\tau_{13} & \tau_{23} & \sigma_3 & D_3\end{bmatrix} = \begin{bmatrix}0 & 0 & 0 & 0\end{bmatrix} \quad \text{on } x_3 = \pm 1 \text{ (open-circuit conditions);} \tag{3.17a}$$

$$\begin{bmatrix}\tau_{13} & \tau_{23} & \sigma_3 & \phi\end{bmatrix} = \begin{bmatrix}0 & 0 & 0 & 0\end{bmatrix} \quad \text{on } x_3 = \pm 1 \text{ (closed-circuit conditions).} \tag{3.17b}$$

At the edges, the following quantities are satisfied:

$$\sigma_2 = u_1 = u_3 = \phi = 0 \quad \text{at } x_2 = 0 \text{ and } x_2 = \theta_\alpha/\sqrt{h/R}. \tag{3.18}$$

4 Asymptotic expansions

Since (3.4)–(3.11) contain terms involving only even powers of $\in$, we therefore asymptotically expand the primary variables in the powers $\in^2$ as follows:

$$f(x_2, x_3, \in, t_0, t_1, \ldots) = f^{(0)}(x_2, x_3, t_0, t_1, \ldots) + \in^2 f^{(1)}(x_2, x_3, t_0, t_1, \ldots) + \in^4 f^{(2)}(x_2, x_3, t_0, t_1, \ldots) + \cdots. \tag{4.1}$$

4.1 Shells with open-circuit surface conditions ($j = 0$)

Substituting (4.1) in (3.4)–(3.11), letting $j = 0$ and collecting coefficients of equal powers of $\in$, we obtain the following sets of recurrence equations for various order problems.

4.1.1 Leading-order problem

After performing nondimensionalization and asymptotic expansion manipulation, we obtain the basic differential equations for the leading-order problem given by

$$u_3^{(0)}{}_{,3} = 0, \quad \phi^{(0)}{}_{,3} = 0, \quad u_1^{(0)}{}_{,3} = 0, \quad u_2^{(0)}{}_{,3} = -u_3^{(0)}{}_{,2} - (\tilde{s}_{44}\tilde{e}_{24})\phi^{(0)}{}_{,2}, \tag{4.2–4.5}$$

$$D_3^{(0)}{}_{,3} = -D_2^{(0)}{}_{,2} = \left[\left(\tilde{s}_{44}\tilde{e}_{24}^2 + \frac{\eta_{22}Q}{e^2}\right) \Big/ \gamma_\theta\right]\phi^{(0)}{}_{,22}, \quad \tau_{13}^{(0)}{}_{,3} = -\bar{Q}_{66}u_1^{(0)}{}_{,22} + \rho_1 \frac{\partial^2 u_1^{(0)}}{\partial t_0^2}, \tag{4.6, 4.7}$$

$$\begin{aligned}\tau_{23}^{(0)}{}_{,3} &= -\bar{Q}_{22}u_2^{(0)}{}_{,22} - \bar{Q}_{22}u_3^{(0)}{}_{,2} - \tilde{b}_2 D_3^{(0)}{}_{,2} + \rho_1 \frac{\partial^2 u_2^{(0)}}{\partial t_0^2},\\ \sigma_3^{(0)}{}_{,3} &= \bar{Q}_{22}u_2^{(0)}{}_{,2} + \bar{Q}_{22}u_3^{(0)} - \tau_{23}^{(0)}{}_{,2} + \tilde{b}_2 D_3^{(0)} + \rho_2 \frac{\partial^2 u_3^{(0)}}{\partial t_0^2}.\end{aligned} \tag{4.8, 4.9}$$

4.1.2 Higher-order problems

The basic differential equations for the higher-order problems are obtained and given by

$$u_{3}^{(k)}{}_{,3} = -\bar{a}_2 u_2^{(k-1)}{}_{,2} - \bar{a}_2 u_3^{(k-1)} + \tilde{e} D_3^{(k-1)} + \tilde{\eta}\sigma_3^{(k-2)},$$
$$\phi^{(k)}{}_{,3} = -\bar{b}_2 u_2^{(k-1)}{}_{,2} - \bar{b}_2 u_3^{(k-1)} - \tilde{c} D_3^{(k-1)} + \tilde{e}\sigma_3^{(k-2)}, \tag{4.10, 4.11}$$

$$u_1^{(k)}{}_{,3} = \tilde{s}_{55}\tau_{13}^{(k-1)}, \quad u_2^{(k)}{}_{,3} = -u_3^{(k)}{}_{,2} - (\tilde{s}_{44}\tilde{e}_{24})\phi^{(k)}{}_{,2} + (1 - x_3\partial_3)u_2^{(k-1)} + \tilde{s}_{44}\tau_{23}^{(k-1)} + (x_3\tilde{s}_{44})\tau_{23}^{(k-2)}, \tag{4.12, 4.13}$$

$$D_3^{(k)}{}_{,3} = -D_2^{(k)}{}_{,2} - (1 + x_3\partial_3)D_3^{(k-1)} = \left[\left(\tilde{s}_{44}\tilde{e}_{24}^2 + \frac{\eta_{22}Q}{e^2}\right)\Big/\gamma_\theta\right]\phi^{(k)}{}_{,22} - (\tilde{s}_{44}\tilde{e}_{24})\tau_{23}^{(k-1)}{}_{,2} - (1 + x_3\partial_3)D_3^{(k-1)}, \tag{4.14}$$

$$\tau_{13}^{(k)}{}_{,3} = -\bar{Q}_{66}u_1^{(k)}{}_{,22} - (1 + x_3\partial_3)\tau_{13}^{(k-1)} + \left[\rho_1\frac{\partial^2}{\partial t_0^2}u_1^{(k)} + 2\rho_1\frac{\partial^2}{\partial t_0\partial t_1}u_1^{(k-1)} + \cdots + \rho_1\left(\frac{\partial^2}{\partial t_0\partial t_k} + \frac{\partial^2}{\partial t_1\partial t_{k-1}} + \cdots + \frac{\partial^2}{\partial t_k\partial t_0}\right)u_1^{(0)}\right], \tag{4.15}$$

$$\tau_{23}^{(k)}{}_{,3} = -\bar{Q}_{22}u_2^{(k)}{}_{,22} - \bar{Q}_{22}u_3^{(k)}{}_{,2} - \tilde{b}_2 D_3^{(k)}{}_{,2} - (2 + x_3\partial_3)\tau_{23}^{(k-1)} - \tilde{a}_2\sigma_3^{(k-1)}{}_{,2} + \left[\rho_1\frac{\partial^2}{\partial t_0^2}u_2^{(k)} + 2\rho_1\frac{\partial^2}{\partial t_0\partial t_1}u_2^{(k-1)} + \cdots + \rho_1\left(\frac{\partial^2}{\partial t_0\partial t_k} + \frac{\partial^2}{\partial t_1\partial t_{k-1}} + \cdots + \frac{\partial^2}{\partial t_k\partial t_0}\right)u_2^{(0)}\right], \tag{4.16}$$

$$\sigma_3^{(k)}{}_{,3} = \bar{Q}_{22}u_2^{(k)}{}_{,2} + \bar{Q}_{22}u_3^{(k)} - \tau_{23}^{(k)}{}_{,2} + \tilde{b}_2 D_3^{(k)} - (-\tilde{a}_2 + 1 + x_3\partial_3)\sigma_3^{(k-1)} + \left[\rho_2\frac{\partial^2}{\partial t_0^2}u_3^{(k)} + 2\rho_2\frac{\partial^2}{\partial t_0\partial t_1}u_3^{(k-1)} + \cdots + \rho_2\left(\frac{\partial^2}{\partial t_0\partial t_k} + \frac{\partial^2}{\partial t_1\partial t_{k-1}} + \cdots + \frac{\partial^2}{\partial t_k\partial t_0}\right)u_3^{(0)}\right], \tag{4.17}$$

where the subscript $k = 1, 2, 3$, etc.

For the previous leading-order ($k = 0$) and higher-order ($k = 1, 2, 3$, etc) problems, the secondary field variables, such as in-surface stresses and electric displacements, can be expressed in terms of the primary variables as follows:

$$\sigma_1^{(k)} = \bar{Q}_{12}u_2^{(k)}{}_{,2} + \bar{Q}_{12}u_3^{(k)} + \tilde{b}_1 D_3^{(k)} + \tilde{a}_1\sigma_3^{(k-1)}, \quad \sigma_2^{(k)} = \bar{Q}_{22}u_2^{(k)}{}_{,2} + \bar{Q}_{22}u_3^{(k)} + \tilde{b}_2 D_3^{(k)} + \tilde{a}_2\sigma_3^{(k-1)}, \tag{4.18, 4.19}$$

$$\tau_{12}^{(k)} = \bar{Q}_{66}u_{1,}^{(k)}{}_{2}, \quad D_1^{(k)} = \tilde{S}_{55}\tilde{e}_{15}\tau_{13}^{(k-1)}, \quad D_2^{(k)} = -\left[\left(\tilde{S}_{44}\tilde{e}_{24}^2 + \frac{\eta_{22}Q}{e^2}\right)\Big/\gamma_\theta\right]\phi_{,2}^{(k)} + \tilde{S}_{44}\tilde{e}_{24}\tau_{23}^{(k-1)}. \tag{4.20.–4.22}$$

The transverse stresses and electric normal displacement on the lateral surfaces are given as

$$\left[\tau_{13}^{(k)} \quad \tau_{23}^{(k)} \quad \sigma_3^{(k)} \quad D_3^{(k)}\right] = [0 \quad 0 \quad 0 \quad 0] \quad \text{on } x_3 = \pm 1. \tag{4.23}$$

Along the edges, the following conditions must be satisfied:

$$\sigma_2^{(k)} = u_1^{(k)} = u_3^{(k)} = \phi_3^{(k)} = 0 \quad \text{at } x_2 = 0 \text{ and } x_2 = \theta_\alpha/\sqrt{h/R}. \tag{4.24}$$

4.2 Shells with closed-circuit surface conditions ($j = 2$)

Substituting (4.1) in (3.4)–(3.11), letting $j = 2$ and collecting coefficients of equal powers of $\in$, we obtain the following sets of recurrence equations for various order problems.

4.2.1 Leading-order problem

The basic differential equations for the leading-order problem given by

$$\phi^{(0)}{}_{,3} = -\bar{b}_2 u_2^{(0)}{}_{,2} - \bar{b}_2 u_3^{(0)} - \tilde{c} D_3^{(0)}, \quad u_2^{(0)}{}_{,3} = -u_3^{(0)}{}_{,2}, \quad D_3^{(0)}{}_{,3} = 0. \tag{4.25–4.27}$$

The other basic equations related to the first derivative of the primary field variables $(u_1^{(0)}, u_3^{(0)}, \tau_{13}^{(0)}, \tau_{23}^{(0)}, \sigma_3^{(0)})$ with respect to the thickness coordinate remain identical to those equations in the cases of open-circuit conditions (i.e., (4.2), (4.4), (4.7)–(4.9)).

4.2.2 Higher-order problems

The basic differential equations for the higher-order problems are obtained and given by

$$\phi^{(k)}{}_{,3} = -\bar{b}_2 u_2^{(k)}{}_{,2} - \bar{b}_2 u_3^{(k)} - \tilde{c} D_3^{(k)} + \tilde{e}\sigma_3^{(k-1)}, \tag{4.28}$$

$$u_2^{(k)}{}_{,3} = -u_3^{(k)}{}_{,2} - (\tilde{S}_{44}\tilde{e}_{24})\phi^{(k-1)}{}_{,2} + (1 - x_3\partial_3)u_2^{(k-1)} + \tilde{S}_{44}\tau_{23}^{(k-1)} + (x_3\tilde{S}_{44})\tau_{23}^{(k-2)}, \tag{4.29}$$

$$D_3^{(k)}{}_{,3} = -D_2^{(k-1)}{}_{,2} - (1 + x_3\partial_3)D_3^{(k-1)} = -\tilde{S}_{44}\tilde{e}_{24}\tau_{23}^{(k-1)}{}_{,2} + \left[\left(\tilde{S}_{44}\tilde{e}_{24}^2 + \frac{\eta_{22}Q}{e^2}\right)\Big/\gamma_\theta\right]\phi^{(k-1)}{}_{,22} - (1 + x_3\partial_3)D_3^{(k-1)}. \tag{4.30}$$

The other differential equations are the same as (4.10), (4.12) and (4.15)–(4.17).

For the previous leading-order and higher-order problems, the expressions of in-surface stresses in terms of the primary variables are the same as (4.18)–(4.20); the expressions of electric displacements are given by

$$D_1^{(k)} = \tilde{s}_{55}\tilde{e}_{15}\tau_{13}^{(k)}, \quad D_2^{(k)} = -\left[\left(\tilde{s}_{44}\tilde{e}_{24}^2 + \frac{\eta_{22}Q}{e^2}\right)\Big/\gamma_\theta\right]\phi^{(k)}{}_{,2} + \tilde{s}_{44}\tilde{e}_{24}\tau_{23}^{(k)}. \tag{4.31, 4.32}$$

The transverse stresses and electric potential on the lateral surfaces are given by

$$\left[\tau_{13}^{(k)} \quad \tau_{23}^{(k)} \quad \sigma_3^{(k)} \quad \phi^{(k)}\right] = \left[0 \quad 0 \quad 0 \quad 0\right] \quad \text{on } x_3 = \pm 1. \tag{4.33}$$

The edge conditions remain the same as those for open-circuit conditions (4.24).

5 Successive integration

5.1 Shells with open-circuit surface conditions ($j = 0$)

5.1.1 Leading-order problem

Examining the sets of asymptotic equations, it is found that the analysis can be carried out by integrating those equations through the thickness direction. We therefore integrate (4.2)–(4.5) to obtain

$$u_3^{(0)} = u_3^0(x_2, t_0, t_1, \ldots), \quad \phi^{(0)} = \phi^0(x_2, t_0, t_1, \ldots), \tag{5.1, 5.2}$$

$$u_1^{(0)} = u_1^0(x_2, t_0, t_1, \ldots), \quad u_2^{(0)} = u_2^0(x_2, t_0, t_1, \ldots) - x_3\, u_3^0{}_{,2} - \tilde{E}_{00}^{24}(x_3)\phi^0{}_{,2}, \tag{5.3, 5.4}$$

where u_1^0, u_2^0, u_3^0 and ϕ^0 represent the displacements and electric potential on the middle surface; also, $\tilde{E}_{00}^{kl}(x_3) = \int_0^{x_3} (\tilde{s}_{ll}\tilde{e}_{kl})\, \mathrm{d}\eta$.

By observing (5.4), we note that the in-surface displacement at the leading-order level is dependent upon the electric potential. Based on the previous study, we may consider (5.1)–(5.4) as the generalized kinematics assumptions of the coupled classical shell theory (CST) for piezoelectric shells with open-circuit surface conditions.

Proceeding to derive the equations of motion at leading-order, we successively integrate (4.6)–(4.9) through the thickness coordinate to obtain

$$D_3^{(0)} = \left[\int_{-1}^{x_3}\left(\tilde{s}_{44}\tilde{e}_{24}^2 + \frac{\eta_{22}\mathcal{Q}}{e^2}\right)\left(\frac{1}{\gamma_\theta}\right)\mathrm{d}\eta\right]\phi^0{}_{,22} = D_3^0, \tag{5.5}$$

$$\tau_{13}^{(0)} = -\left(\int_{-1}^{x_3}\overline{Q}_{66}\mathrm{d}\eta\right)u_1^0{}_{,22} + \left(\int_{-1}^{x_3}\rho_1\mathrm{d}\eta\right)\frac{\partial^2 u_1^0}{\partial t_0^2}, \tag{5.6}$$

$$\begin{aligned}\tau_{23}^{(0)} = &-\int_{-1}^{x_3}\left[\overline{Q}_{22}\left(u_2^0{}_{,22} - \eta u_3^0{}_{,222} - \tilde{E}_{00}^{24}\phi^0{}_{,222}\right) + \overline{Q}_{22}u_{3,2}^0 + \tilde{b}_2 D_{3,2}^0\right]\mathrm{d}\eta\\ &+\left(\int_{-1}^{x_3}\rho_1\mathrm{d}\eta\right)\frac{\partial^2 u_2^0}{\partial t_0^2} - \left(\int_{-1}^{x_3}\rho_1\eta\mathrm{d}\eta\right)\frac{\partial^2 u_{3,2}^0}{\partial t_0^2} - \left(\int_{-1}^{x_3}\rho_1\tilde{E}_{00}^{24}\mathrm{d}\eta\right)\frac{\partial^2\phi^0{}_{,2}}{\partial t_0^2},\end{aligned} \tag{5.7}$$

$$\begin{aligned}\sigma_3^{(0)} = &\int_{-1}^{x_3}\left[\overline{Q}_{22}\left(u_2^0{}_{,2} - \eta u_3^0{}_{,22} - \tilde{E}_{00}^{24}\phi^0{}_{,22}\right) + \overline{Q}_{22}u_3^0 + \tilde{b}_2 D_3^0\right]\mathrm{d}\eta\\ &+\int_{-1}^{x_3}(x_3-\eta)\left[\overline{Q}_{22}\left(u_2^0{}_{,222} - \eta u_3^0{}_{,2222} - \tilde{E}_{00}^{24}\phi^0{}_{,2222}\right) + \overline{Q}_{22}u_3^0{}_{,22} + \tilde{b}_2 D_3^0{}_{,22}\right]\mathrm{d}\eta\\ &+\left(\int_{-1}^{x_3}\rho_2\mathrm{d}\eta\right)\frac{\partial^2 u_3^0}{\partial t_0^2} - \left(\int_{-1}^{x_3}(x_3-\eta)\,\rho_1\mathrm{d}\eta\right)\frac{\partial^2 u_{2,2}^0}{\partial t_0^2} + \left(\int_{-1}^{x_3}(x_3-\eta)\,\rho_1\eta\mathrm{d}\eta\right)\frac{\partial^2 u_3^0{}_{,22}}{\partial t_0^2}\\ &+\left(\int_{-1}^{x_3}(x_3-\eta)\,\rho_1\tilde{E}_{00}^{24}\mathrm{d}\eta\right)\frac{\partial^2\phi^0{}_{,22}}{\partial t_0^2}.\end{aligned} \tag{5.8}$$

After imposing the lateral boundary conditions at $x_3 = 1$, we obtain the governing equations for the leading-order problem as follows:

$$K_{11}u_1^0 = -I_{10}\frac{\partial^2 u_1^0}{\partial t_0^2}, \quad K_{22}u_2^0 + K_{23}u_3^0 + K_{24}\phi^0 = -I_{10}\frac{\partial^2 u_2^0}{\partial t_0^2} + I_{11}\frac{\partial^2 u_{3,2}^0}{\partial t_0^2} + I_{10}^{24}\frac{\partial^2\phi^0{}_{,2}}{\partial t_0^2}, \tag{5.9, 5.10}$$

$$K_{32}u_2^0 + K_{33}u_3^0 + K_{34}\phi^0 = -I_{20}\frac{\partial^2 u_3^0}{\partial t_0^2} - I_{11}\frac{\partial^2 u_{2,2}^0}{\partial t_0^2} + I_{12}\frac{\partial^2 u_3^0{}_{,22}}{\partial t_0^2} + I_{11}^{24}\frac{\partial^2\phi^0{}_{,22}}{\partial t_0^2}, \quad K_{44}\phi^0 = 0, \tag{5.11–5.12}$$

in which

$$\begin{aligned}&K_{11} = -\bar{A}_{66}\partial_{22}, \quad K_{22} = -\bar{A}_{22}\partial_{22}, \quad K_{23} = \bar{B}_{22}\partial_{222} - \bar{A}_{22}\partial_2,\\ &K_{24} = \left(\bar{E}_{22}^{24} - \tilde{F}_{32}^{24}\right)\partial_{222}, \quad K_{32} = -\bar{B}_{22}\partial_{222} + \bar{A}_{22}\partial_2, \quad K_{33} = \bar{D}_{22}\partial_{2222} - 2\bar{B}_{22}\partial_{22} + \bar{A}_{22},\\ &K_{34} = \left(\bar{G}_{22}^{24} - \tilde{H}_{32}^{24}\right)\partial_{2222} - \left(\bar{E}_{22}^{24} - \tilde{F}_{32}^{24}\right)\partial_{22}, \quad K_{44} = \bar{F}^{24}\partial_{22};\end{aligned}$$

$$\begin{bmatrix}\hat{A}_{ij}\\ \tilde{A}_{ij}\\ \overline{A}_{ij}\end{bmatrix}=\int_{-1}^{1}\begin{bmatrix}\hat{Q}_{ij}\\ \tilde{Q}_{ij}\\ \overline{Q}_{ij}\end{bmatrix}\mathrm{d}x_3,\quad \begin{bmatrix}\hat{B}_{ij}\\ \tilde{B}_{ij}\\ \overline{B}_{ij}\end{bmatrix}=\int_{-1}^{1}x_3\begin{bmatrix}\hat{Q}_{ij}\\ \tilde{Q}_{ij}\\ \overline{Q}_{ij}\end{bmatrix}\mathrm{d}x_3,\quad \begin{bmatrix}\hat{D}_{ij}\\ \tilde{D}_{ij}\\ \overline{D}_{ij}\end{bmatrix}=\int_{-1}^{1}x_3^2\begin{bmatrix}\hat{Q}_{ij}\\ \tilde{Q}_{ij}\\ \overline{Q}_{ij}\end{bmatrix}\mathrm{d}x_3,$$

$$\begin{bmatrix}\hat{E}_{ij}^{kl}\\ \tilde{E}_{ij}^{kl}\\ \overline{E}_{ij}^{kl}\end{bmatrix}=\int_{-1}^{1}\begin{bmatrix}\hat{Q}_{ij}\\ \tilde{Q}_{ij}\\ \overline{Q}_{ij}\end{bmatrix}\int_0^{x_3}(\tilde{s}_{ll}\tilde{e}_{kl})\mathrm{d}\eta\mathrm{d}x_3,\quad \begin{bmatrix}\hat{F}_{3i}^{kl}\\ \tilde{F}_{3i}^{kl}\\ \overline{F}_{3i}^{kl}\end{bmatrix}=\int_{-1}^{1}\begin{bmatrix}\hat{b}_i\\ \tilde{b}_i\\ \overline{b}_i\end{bmatrix}\int_{-1}^{x_3}\left(\frac{1}{\gamma_\theta}\right)\left(\tilde{s}_{ll}\tilde{e}_{kl}^2+\frac{\eta_{kk}Q}{e^2}\right)\mathrm{d}\eta\mathrm{d}x_3,$$

$$\begin{bmatrix}\hat{F}_{3i}\\ \tilde{F}_{3i}\\ \overline{F}_{3i}\end{bmatrix}=\int_{-1}^{1}\begin{bmatrix}\hat{b}_i\\ \tilde{b}_i\\ \overline{b}_i\end{bmatrix}\mathrm{d}x_3,\quad \begin{bmatrix}\hat{F}^{kl}\\ \tilde{F}^{kl}\\ \overline{F}^{kl}\end{bmatrix}=\int_{-1}^{1}\left(\tilde{s}_{ll}\tilde{e}_{kl}^2+\frac{\eta_{kk}Q}{e^2}\right)\begin{bmatrix}\gamma_\theta\\ 1\\ 1/\gamma_\theta\end{bmatrix}\mathrm{d}x_3,$$

$$\begin{bmatrix}\hat{G}_{ij}^{kl}\\ \tilde{G}_{ij}^{kl}\\ \overline{G}_{ij}^{kl}\end{bmatrix}=\int_{-1}^{1}x_3\begin{bmatrix}\hat{Q}_{ij}\\ \tilde{Q}_{ij}\\ \overline{Q}_{ij}\end{bmatrix}\int_0^{x_3}(\tilde{s}_{ll}\tilde{e}_{kl})\mathrm{d}\eta\mathrm{d}x_3,\quad \begin{bmatrix}\hat{H}_{3i}^{kl}\\ \tilde{H}_{3i}^{kl}\\ \overline{H}_{3i}^{kl}\end{bmatrix}=\int_{-1}^{1}x_3\begin{bmatrix}\hat{b}_i\\ \tilde{b}_i\\ \overline{b}_i\end{bmatrix}\int_{-1}^{x_3}\left(\frac{1}{\gamma_\theta}\right)\left(\tilde{s}_{ll}\tilde{e}_{kl}^2+\frac{\eta_{kk}Q}{e^2}\right)\mathrm{d}\eta\mathrm{d}x_3,$$

$$\begin{bmatrix}\hat{H}_{3i}\\ \tilde{H}_{3i}\\ \overline{H}_{3i}\end{bmatrix}=\int_{-1}^{1}x_3\begin{bmatrix}\hat{b}_i\\ \tilde{b}_i\\ \overline{b}_i\end{bmatrix}\mathrm{d}x_3,\quad (i,j=1,2,6)\text{ and }(k,l)=(2,4)\text{ or }(1,5);$$

$$I_{10}=\int_{-1}^{1}\rho_1\mathrm{d}x_3,\quad I_{11}=\int_{-1}^{1}\rho_1x_3\mathrm{d}x_3,\quad I_{12}=\int_{-1}^{1}\rho_1x_3^2\mathrm{d}x_3,$$

$$I_{10}^{24}=\int_{-1}^{1}\rho_1\tilde{E}_{00}^{24}(x_3)\mathrm{d}x,\quad I_{11}^{24}=\int_{-1}^{1}\rho_1x_3\tilde{E}_{00}^{24}(x_3)\mathrm{d}x_3,\quad I_{20}=\int_{-1}^{1}\rho_2\mathrm{d}x_3.$$

The equations of motion of the leading-order problem (5.9)–(5.12) with the edge boundary conditions (4.24) constitute a well-posed eigenvalue problem which can be readily solved. Once u_1^0, u_2^0, u_3^0, and ϕ^0 have been determined, the leading-order solutions of the other modal variables of the electric and mechanical fields can be obtained by (4.18)–(4.22) and (5.1)–(5.8).

5.1.2 Higher-order problems

Proceeding to order ϵ^{2k} ($k=1,2,3$, etc) and integrating (4.10)–(4.13) through the thickness coordinate, we obtain

$$u_3^k=u_3^k(x_2,t_o,t_1,t_2,\ldots)+\varphi_{3k}(x_2,x_3,t_0,t_1,t_2,\ldots),$$
$$\phi^{(k)}=\phi^k(x_2,t_o,t_1,t_2,\ldots)+\varphi_{4k}(x_2,x_3,t_0,t_1,t_2,\ldots),\qquad(5.13,\,5.14)$$

$$u_1^{(k)}=u_1^k(x_2,t_o,t_1,t_2,\ldots)+\varphi_{1k}(x_2,x_3,t_0,t_1,t_2,\ldots),$$
$$u_2^{(k)}=u_2^k(x_2,t_o,t_1,t_2,\ldots)-x_3u_{3,2}^k-\tilde{E}_{00}^{24}(x_3)\phi^k{}_{,2}+\varphi_{2k}(x_2,x_3,t_0,t_1,t_2,\ldots),\qquad(5.15,\,5.16)$$

where u_1^k, u_2^k, u_3^k and ϕ^k represent the modifications to the modal elastic displacements and electric potential on the middle surface; $\varphi_{1k}=0$; φ_{2k}, φ_{3k} and φ_{4k} are the relevant functions and their explicit expressions are given in the Appendix.

After integrating (4.14)–(4.17) through the thickness coordinate, using (5.13)–(5.16) and the lateral boundary conditions (4.23) and following a similar derivation as for the leading-order problem, we obtain the governing equations for the higher-order problems as follows:

$$K_{11}u_1^k=f_{1k}(x_2,1,t_0,t_1,\ldots)-I_{10}\frac{\partial^2u_1^k}{\partial t_0^2}\qquad(5.17)$$

$$K_{22}u_2^k+K_{23}u_3^k+K_{24}\phi^k=f_{2k}(x_2,1,t_0,t_1,\ldots)-I_{10}\frac{\partial^2u_2^k}{\partial t_0^2}+I_{11}\frac{\partial^2u_{3,2}^k}{\partial t_0^2}+I_{10}^{24}\frac{\partial^2\phi^k{}_{,2}}{\partial t_0^2},\qquad(5.18)$$

$$K_{32}u_2^k + K_{33}u_3^k + K_{34}\phi^k = f_{3k}(x_2, 1, t_0, t_1, \ldots) + \frac{\partial f_{2k}(x_2, 1, t_0, t_1, \ldots)}{\partial x_2} - I_{20}\frac{\partial^2 u_3^k}{\partial t_0^2} - I_{11}\frac{\partial^2 u_{2,2}^k}{\partial t_0^2} + I_{12}\frac{\partial^2 u_{3,22}^k}{\partial t_0^2} + I_{11}^{24}\frac{\partial^2 \phi^k{}_{,22}}{\partial t_0^2}, \tag{5.19}$$

$$K_{44}\phi^k = f_{4k}(x_2, 1, t_0, t_1, \ldots), \tag{5.20}$$

where $f_{1k} = 0$; f_{2k}, f_{3k} and f_{4k} are the nonhomogenous terms that can be calculated from the lower-order solutions. The explicit expressions of $f_{lk}(l = 2, 3, 4)$ are given in the Appendix.

With the appropriate edge boundary conditions, the higher-order modifications for the natural frequencies, their corresponding eigenvectors (i.e., u_1^k, u_2^k, u_3^k and ϕ^k) and other modal variables can be readily obtained.

It is noted that the governing equations pertaining to the higher-order problems are the same as those of the leading-order problem, except for the nonhomogenous terms. In view of the recursive property, a solution methodology applied for solving the leading-order problem can be repeatedly applied for solving the higher-order problems. Hence, the present asymptotic solutions can be obtained in a hierarchic manner.

5.2 Shells with closed-circuit surface conditions ($j = 2$)

5.2.1 Leading-order problem

Following a derivation similar to that of Sect. 5.1 and performing successive integration of those basic differential equations through the thickness direction (i.e., (4.2), (4.4), (4.26) and (4.27)), we obtain

$$u_3^{(0)} = u_3^0(x_2, t_0, t_1, \ldots), \quad u_1^{(0)} = u_1^0(x_2, t_0, t_1, \ldots), \quad u_2^{(0)} = u_2^0(x_2, t_0, t_1, \ldots) - x_3 u_{3,2}^0, \tag{5.21–5.23}$$

$$D_3^{(0)} = D_3^0(x_2, t_0, t_1 \ldots), \tag{5.24}$$

where u_1^0, u_2^0, u_3^0 and D_3^0 represent the displacements and normal electric displacement on the middle surface.

Equations (5.21)–(5.24) may be considered as the generalized kinematics assumptions of the coupled CST for piezoelectric shells with closed-circuit surface conditions.

Integrating the basic differential equations relative to the transverse stresses (4.7)–(4.9) and electric potential (4.25) through the thickness coordinate and using the lateral boundary conditions on $x_3 = \pm 1$, we obtain

$$K_{11}u_1^0 = -I_{10}\frac{\partial^2 u_1^0}{\partial t_0^2}, \quad K_{22}u_2^0 + K_{23}u_3^0 + L_{24}D_3^0 = -I_{10}\frac{\partial^2 u_2^0}{\partial t_0^2} + I_{11}\frac{\partial^2 u_{3,2}^0}{\partial t_0^2}, \tag{5.25, 5.26}$$

$$K_{32}u_2^0 + K_{33}u_3^0 + L_{34}D_3^0 = -I_{11}\frac{\partial^2 u_{2,2}^0}{\partial t_0^2} + I_{12}\frac{\partial^2 u_{3,22}^0}{\partial t_0^2} - I_{20}\frac{\partial^2 u_3^0}{\partial t_0^2}, \quad L_{42}u_2^0 + L_{43}u_3^0 + L_{44}D_3^0 = 0, \tag{5.27, 5.28}$$

in which K_{ij} were defined as previously for open-circuit conditions, and

$$L_{24} = -\tilde{F}_{32}\partial_2, \quad L_{34} = -\tilde{H}_{32}\partial_{22} + \tilde{F}_{32}, \quad L_{42} = -\tilde{F}_{32}\partial_2,$$
$$L_{43} = \tilde{H}_{32}\partial_{22} - \tilde{F}_{32}, \quad L_{44} = -E_0, \quad E_0 = \int_{-1}^{1} \tilde{c}\, \mathrm{d}x_3.$$

The equations of motion (5.25)–(5.28) for the leading-order problem combined with the edge boundary conditions (4.24) constitute a well-posed eigenvalue problem which can be readily solved. Once u_1^0, u_2^0, u_3^0 and D_3^0 have been determined, the leading-order solutions of other variables of the electric and mechanical fields can be obtained as before.

5.2.2 Higher-order problems

Proceeding to order $\in^{2k}$ ($k = 1, 2, 3$, etc) and integrating (4.10), (4.12), (4.29) and (4.30) through the thickness coordinate, we readily obtain

$$u_3^{(k)} = u_3^k(x_2, t_0, t_1, \ldots) + \psi_{3k}(x_2, x_3, t_0, t_1, \ldots), \quad D_3^{(k)} = D_3^k(x_2, t_0, t_1, \ldots) + \psi_{4k}(x_2, x_3, t_0, t_1, \ldots), \tag{5.29, 5.30}$$

$$u_1^{(k)} = u_1^k(x_2, t_0, t_1, \ldots) + \psi_{1k}(x_2, x_3, t_0, t_1, \ldots), \quad u_2^{(k)} = u_2^k(x_2, t_0, t_1, \ldots) - x_3 u_{3,2}^k + \psi_{2k}(x_2, x_3, t_0, t_1, \ldots), \tag{5.31, 5.32}$$

where u_1^k, u_2^k, u_3^k and D_3^k represent the modifications to the modal elastic displacements and electric displacement on the middle surface; $\psi_{1k} = 0$; ψ_{2k}, ψ_{3k} and ψ_{4k} are the relevant functions and their explicit expressions are given in the Appendix.

After integrating the basic differential equations through the thickness coordinate and using the lateral boundary conditions, we obtain the governing equations for the higher-order problems as follows:

$$K_{11}u_1^k = g_{1k}(x_2, 1, t_0, t_1, \ldots) - I_{10}\frac{\partial^2 u_1^k}{\partial t_0^2}, \tag{5.33, 5.34}$$

$$K_{22}u_2^k + K_{23}u_3^k + L_{24}D_3^k = g_{2k}(x_2, 1, t_0, t_1 \ldots) - I_{10}\frac{\partial^2 u_2^k}{\partial t_0^2} + I_{11}\frac{\partial^2 u_{3,2}^k}{\partial t_0^2},$$

$$K_{32}u_2^k + K_{33}u_3^k + L_{34}D_3^k = g_{3k}(x_2, 1, t_0, t_1, \ldots) + \frac{\partial g_{2k}(x_2, 1, t_0, t_1, \ldots)}{\partial x_2} - I_{11}\frac{\partial^2 u_{2,2}^k}{\partial t_0^2} + I_{12}\frac{\partial^2 u_{3,22}^k}{\partial t_0^2} - I_{20}\frac{\partial^2 u_3^k}{\partial t_0^2}, \tag{5.35}$$

$$L_{42}u_2^k + L_{43}u_3^k + L_{44}D_3^k = g_{4k}(x_2, 1, t_0, t_1, \ldots), \tag{5.36}$$

where $g_{1k} = 0$; g_{2k}, g_{3k} and g_{4k} are the nonhomogenous terms which can be calculated from the lower-order solutions. Explicit expressions for $g_{lk}(l = 2, 3, 4)$ are given in the Appendix.

With the appropriate edge boundary conditions, the higher-order modifications (i.e., u_1^k, u_2^k, u_3^k and D_3^k) and the other modal variables can be readily obtained using the same solution methodology as was used for the leading-order problem.

6 Applications to benchmark problems

Cylindrical bending vibration problems of simply supported, multilayered and functionally graded piezoelectric cylindrical shells (Fig. 1) with open-circuit and closed-circuit surface conditions are studied using the present asymptotic formulations.

6.1 Shells with open-circuit surface conditions (j = 0)

The governing equations of the leading-order problem ((5.9)–(5.12)) can be readily solved by letting

$$u_1^0 = \sum_{n=1}^{\infty} u_{1n}^0 \sin\tilde{n}x_2 \cos(\omega t_0 - \vartheta), \quad u_2^0 = \sum_{n=1}^{\infty} u_{2n}^0 \cos\tilde{n}x_2 \cos(\omega t_0 - \vartheta), \tag{6.1–6.2}$$

$$u_3^0 = \sum_{n=1}^{\infty} u_{3n}^0 \sin\tilde{n}x_2 \cos(\omega t_0 - \vartheta), \quad \phi^0 = \sum_{n=1}^{\infty} \phi_n^0 \sin\tilde{n}x_2 \cos(\omega t_0 - \vartheta), \tag{6.3–6.4}$$

where $\tilde{n} = n/\sqrt{h/R}$ and n is a positive integer; ω denotes the circular frequency of the motion. The phase angle ϑ is a function of the time scales (t_1, t_2, t_3, etc), but not of t_0.

Substituting (6.1)–(6.4) in (5.9)–(5.12) gives

$$\begin{bmatrix} k_{11} & 0 & 0 & 0 \\ 0 & k_{22} & k_{23} & k_{24} \\ 0 & k_{32} & k_{33} & k_{34} \\ 0 & 0 & 0 & k_{44} \end{bmatrix} \begin{Bmatrix} u_{1n}^0 \\ u_{2n}^0 \\ u_{3n}^0 \\ \phi_n^0 \end{Bmatrix} = \omega^2 \begin{bmatrix} I_{10} & 0 & 0 & 0 \\ 0 & I_{10} & -\tilde{n} I_{11} & -\tilde{n} I_{10}^{24} \\ 0 & -\tilde{n} I_{11} & (I_{20} + \tilde{n}^2 I_{12}) & \tilde{n} I_{11}^{24} \\ 0 & 0 & 0 & 0 \end{bmatrix} \begin{Bmatrix} u_{1n}^0 \\ u_{2n}^0 \\ u_{3n}^0 \\ \phi_n^0 \end{Bmatrix}, \tag{6.5}$$

where

$$k_{11} = \tilde{n}^2 \bar{A}_{66}, \quad k_{22} = \tilde{n}^2 \bar{A}_{22}, \quad k_{23} = -\tilde{n}^3 \bar{B}_{22} - \tilde{n} \bar{A}_{22},$$
$$k_{24} = -\tilde{n}^3 (\bar{E}_{22}^{24} - \tilde{F}_{32}^{24}), \quad k_{32} = -\tilde{n}^3 \bar{B}_{22} - \tilde{n} \bar{A}_{22}, \quad k_{33} = \tilde{n}^4 \bar{D}_{22} + 2\tilde{n} \bar{B}_{22} + \bar{A}_{22},$$
$$k_{34} = \tilde{n}^4 \left(\bar{G}_{22}^{24} - \tilde{H}_{32}^{24} \right) + \tilde{n}^2 \left(\bar{E}_{22}^{24} - \tilde{F}_{32}^{24} \right), \quad k_{44} = -\tilde{n}^2 \bar{F}^{24}.$$

The electric potential ϕ_n^0 can be determined from (6.5) and is given by

$$\phi_n^0 = 0 \tag{6.6}$$

According to (6.5)–(6.6), we can rewrite (6.5) in the form

$$\begin{bmatrix} k_{11} & 0 & 0 \\ 0 & k_{22} & k_{23} \\ 0 & k_{32} & k_{33} \end{bmatrix} \begin{Bmatrix} u_{1n}^0 \\ u_{2n}^0 \\ u_{3n}^0 \end{Bmatrix} = \omega^2 \begin{bmatrix} I_{10} & 0 & 0 \\ 0 & I_{10} & -\tilde{n} I_{11} \\ 0 & -\tilde{n} I_{11} & (I_{20} + \tilde{n}^2 I_{12}) \end{bmatrix} \begin{Bmatrix} u_{1n}^0 \\ u_{2n}^0 \\ u_{3n}^0 \end{Bmatrix}. \tag{6.7}$$

Equation (6.7) is an eigenvalue problem. A nontrivial solution of (6.7) exists if the determinant of the coefficient matrix vanishes. Hence, the natural frequencies at leading order for a fixed n can be obtained from

$$\begin{vmatrix} k_{11} - \omega^2 I_{10} & 0 & 0 \\ 0 & k_{22} - \omega^2 I_{10} & k_{23} + \omega^2 \tilde{n} I_{11} \\ 0 & k_{32} + \omega^2 \tilde{n} I_{11} & k_{33} - \omega^2 (I_{20} + \tilde{n}_2 I_{12}) \end{vmatrix} = 0. \tag{6.8}$$

The modal displacements are normalized to render the asymptotic solution for various orders unique. They are given by

$$[(u_{1n}^0 + \epsilon^2 u_{1n}^1 + \epsilon^4 u_{1n}^2 + \cdots) \quad (u_{2n}^0 + \epsilon^2 u_{2n}^1 + \epsilon^4 u_{2n}^2 + \cdots) \quad (u_{3n}^0 + \epsilon^2 u_{3n}^1 + \epsilon^4 u_{3n}^2 + \cdots)]$$
$$[(u_{1n}^0 + \epsilon^2 u_{1n}^1 + \epsilon^4 u_{1n}^2 + \cdots) \quad (u_{2n}^0 + \epsilon^2 u_{2n}^1 + \epsilon^4 u_{2n}^2 + \cdots) \quad (u_{3n}^0 + \epsilon^2 u_{3n}^1 + \epsilon^4 u_{3n}^2 + \cdots)]^T = 1. \tag{6.9}$$

The orthonormality conditions at each level are

$$\epsilon^0\text{-order: } (u_{1n}^0)^2 + (u_{2n}^0)^2 + (u_{3n}^0)^2 = 1; \tag{6.10}$$

$$\epsilon^2\text{-order: } (u_{1n}^0)^2 + (u_{2n}^0)^2 + (u_{3n}^0)^2 = 1, \quad u_{1n}^0 u_{1n}^1 + u_{2n}^0 u_{2n}^1 + u_{3n}^0 u_{3n}^1 = 0; \tag{6.11}$$

$$\begin{aligned} \epsilon^4\text{-order: } & (u_{1n}^0)^2 + (u_{2n}^0)^2 + (u_{3n}^0)^2 = 1, \quad u_{1n}^0 u_{1n}^1 + u_{2n}^0 u_{2n}^1 + u_{3n}^0 u_{3n}^1 = 0; \\ & (u_{1n}^1)^2 + 2u_{1n}^0 u_{1n}^2 + (u_{2n}^1)^2 + 2u_{2n}^0 u_{2n}^2 + (u_{3n}^1)^2 + 2u_{3n}^0 u_{3n}^2 = 0; \text{ etc.} \end{aligned} \tag{6.12}$$

At the ϵ^0-order level, the normalized eigenvectors corresponding to $\omega_i (i = 1, 2, 3)$ for fixed n are written as $\{(u_{1n}^0)_i \quad (u_{2n}^0)_i \quad (u_{3n}^0)_i\}^T$. Once they have been determined, the corresponding modal variables of the elastic and electric fields at leading-order can then be calculated.

Carrying on the solution to ϵ^2-order, we find that the nonhomogeneous terms for fixed values of n are

$$f_{21}(x_2, 1) = \left(\hat{f}_{21}(1) \frac{\partial \vartheta_i}{\partial t_1} + \tilde{f}_{21}(1) \right) \cos \tilde{n} x_2 \cos(\omega_i t_0 - \vartheta_i), \tag{6.13}$$

$$f_{31}(x_2, 1) = \left(\hat{f}_{31}(1) \frac{\partial \vartheta_i}{\partial t_1} + \tilde{f}_{31}(1) \right) \sin \tilde{n} x_2 \cos(\omega_i t_0 - \vartheta_i), \tag{6.14}$$

$$f_{41}(x_2,1)=\left(\hat{f}_{41}(1)\frac{\partial\vartheta_i}{\partial t_1}+\tilde{f}_{41}(1)\right)\sin\tilde{n}x_2\cos(\omega_i t_0-\vartheta_i), \tag{6.15}$$

where $\hat{f}_{j1}$ and $\tilde{f}_{j1}(j=2,3,4)$ are the relevant coefficients.

In view of the recurrence of the equations, the ϵ^2-order solution can be obtained by letting

$$u_1^1=u_{1n}^1\sin\tilde{n}x_2\cos(\omega_i t_0-\vartheta_i),\quad u_2^1=u_{2n}^1\cos\tilde{n}x_2\cos(\omega_i t_0-\vartheta_i), \tag{6.16, 6.17}$$

$$u_3^1=u_{3n}^1\sin\tilde{n}x_2\cos(\omega_i t_0-\vartheta_i),\quad \phi^1=\phi_n^1\sin\tilde{n}x_2\cos(\omega_i t_0-\vartheta_i). \tag{6.18, 6.19}$$

Substituting (6.13)–(6.15) and (6.16)–(6.19) in (5.17)–(5.20) gives

$$\begin{bmatrix} k_{11}-I_{10}\omega_i^2 & 0 & 0 & 0\\ 0 & k_{22}-I_{10}\omega_i^2 & k_{23}+\tilde{n}I_{11}\omega_i^2 & k_{24}+\tilde{n}I_{10}^{24}\omega_i^2\\ 0 & k_{32}+\tilde{n}I_{11}\omega_i^2 & k_{33}-(I_{20}+\tilde{n}^2I_{12})\omega_i^2 & k_{34}-\tilde{n}^2I_{11}^{24}\omega_i^2\\ 0 & 0 & 0 & k_{44}\end{bmatrix}\begin{Bmatrix} u_{1n}^1\\ u_{2n}^1\\ u_{3n}^1\\ \phi_n^1\end{Bmatrix}$$

$$=\begin{Bmatrix} 0\\ \hat{f}_{21}(1)\dfrac{\partial\vartheta_i}{\partial t_1}+\tilde{f}_{21}(1)\\ [\hat{f}_{31}(1)-\tilde{n}\hat{f}_{21}(1)]\dfrac{\partial\vartheta_i}{\partial t_1}+[\tilde{f}_{31}(1)-\tilde{n}\tilde{f}_{21}(1)]\\ \tilde{f}_{41}(1)\end{Bmatrix}. \tag{6.20}$$

Following a solution procedure similar to that of the leading-order level, we obtain

$$\phi_n^1=\frac{\tilde{f}_{41}(1)}{k_{44}}. \tag{6.21}$$

Equation (6.21) can then be rewritten as

$$\begin{bmatrix} k_{11}-I_{10}\omega_i^2 & 0 & 0\\ 0 & k_{22}-I_{10}\omega_i^2 & k_{23}+\tilde{n}I_{11}\omega_i^2\\ 0 & k_{32}+\tilde{n}I_{11}\omega_i^2 & k_{33}-\left(I_{20}+\tilde{n}^2I_{12}\right)\omega_i^2\end{bmatrix}\begin{Bmatrix} u_{1n}^1\\ u_{2n}^1\\ u_{3n}^1\end{Bmatrix}=\begin{Bmatrix} 0\\ \hat{f}_{21}(1)\dfrac{\partial\vartheta_i}{\partial t_1}+\tilde{h}_{21}(1)\\ \left[\hat{f}_{31}(1)-\tilde{n}\hat{f}_{21}(1)\right]\dfrac{\partial\vartheta_i}{\partial t_1}+\left[\tilde{h}_{31}(1)-\tilde{n}\tilde{f}_{21}(1)\right]\end{Bmatrix}, \tag{6.22}$$

where $\tilde{h}_{21}(1)=\tilde{f}_{21}(1)-\left(k_{24}+\tilde{n}I_{10}^{24}\omega_i^2\right)\phi_n^1$, $\tilde{h}_{31}(1)=\tilde{f}_{31}(1)-\left(k_{34}-\tilde{n}^2I_{11}^{24}\omega_i^2\right)\phi_n^1$.
The solvability condition for (6.22) is given by

$$\left(u_{2n}^0\right)_i\left\{\hat{f}_{21}(1)\frac{\partial\vartheta_i}{\partial t_1}+\tilde{h}_{21}(1)\right\}+\left(u_{3n}^0\right)_i\left\{\left[\hat{f}_{31}(1)-\tilde{n}\hat{f}_{21}(1)\right]\frac{\partial\vartheta_i}{\partial t_1}+\left[\tilde{h}_{31}(1)-\tilde{n}\tilde{f}_{21}(1)\right]\right\}=0. \tag{6.23}$$

Equation (6.22) is solvable if and only if the solvability condition (6.23) is satisfied. Collecting the terms of $\partial\vartheta_i/\partial t_1$, we may rewrite Eq. (6.23) as

$$\left\{\left(u_{2n}^0\right)_i\hat{f}_{21}(1)+\left(u_{3n}^0\right)_i\left[\hat{f}_{31}(1)-\tilde{n}\hat{f}_{21}(1)\right]\right\}\frac{\partial\vartheta_i}{\partial t_1}+\left\{\left(u_{2n}^0\right)_i\tilde{h}_{21}(1)+\left(u_{3n}^0\right)_i\left[\tilde{h}_{31}(1)-\tilde{n}\tilde{f}_{21}(1)\right]\right\}=0. \tag{6.24}$$

Since the coefficients of $(\partial\vartheta_i/\partial t_1)$ in (6.24) are constants, the dependence of ϑ_i upon t_1 can then be determined as

$$\vartheta_i=-\lambda_i t_1+\overline{\vartheta}\,(t_2,t_3,\ldots), \tag{6.25}$$

where the λ_i are certain constants which are given as $\lambda_i=\frac{\left(u_{2n}^0\right)_i\tilde{h}_{21}(1)+\left(u_{3n}^0\right)_i\left[\tilde{h}_{31}(1)-\tilde{n}\tilde{f}_{21}(1)\right]}{\left(u_{2n}^0\right)_i\hat{f}_{21}(1)+\left(u_{3n}^0\right)_i\left[\hat{f}_{31}(1)-\tilde{n}\hat{f}_{21}(1)\right]}$.

With (6.25) and the relation $t_1=\epsilon^2\,t_0=(h/R)t_0$, the time functions of all field variables are now expressed in terms of $\cos\left[(\omega+\lambda h/R)t_0-\overline{\vartheta}\right]$. Therefore, the natural frequencies at the ϵ^2-order level have been modified to

$$\omega_i+\lambda_i\frac{h}{R}\quad(i=1,2,3). \tag{6.26}$$

Substituting (6.25) in (6.22) yields

$$\begin{bmatrix} k_{11}-I_{10}\omega_i^2 & 0 & 0 \\ 0 & k_{22}-I_{10}\omega_i^2 & k_{23}+\tilde{n}I_{11}\omega_i^2 \\ 0 & k_{32}+\tilde{n}I_{11}\omega_i^2 & k_{33}-\left(I_{20}+\tilde{n}^2I_{12}\right)\omega_i^2 \end{bmatrix} \begin{Bmatrix} u_{1n}^1 \\ u_{2n}^1 \\ u_{3n}^1 \end{Bmatrix} = \begin{Bmatrix} 0 \\ -\hat{f}_{21}(1)\lambda_i+\tilde{h}_{21}(1) \\ -\left[\hat{f}_{31}(1)-\tilde{n}\hat{f}_{21}(1)\right]\lambda_i+\left[\hat{h}_{31}(1)-\tilde{n}\tilde{f}_{21}(1)\right] \end{Bmatrix}. \tag{6.27}$$

The variables of u_{1n}^1, u_{2n}^1 and u_{3n}^1 can be determined from (6.27) and the modifications of the other modal variables of the $\in^2$-order are subsequently determined as before. The solution process can be repeatedly applied for various order problems and the asymptotic solutions can be obtained hierarchically.

6.2 Shells with closed-circuit surface conditions ($j = 2$)

The governing equations of the leading-order problem ((5.25)–(5.28)) can also be solved by letting u_1^0, u_2^0, and u_3^0, be of the same form as (6.1)–(6.3) and

$$D_3^0 = \sum_{n=1}^{\infty} D_{3n}^0 \sin\tilde{n}x_2\cos(\omega t_0-\vartheta). \tag{6.28}$$

Substituting (6.1)–(6.3) and (6.28) in (5.25)–(5.28) gives

$$\begin{bmatrix} k_{11} & 0 & 0 & 0 \\ 0 & k_{22} & k_{23} & l_{24} \\ 0 & k_{32} & k_{33} & l_{34} \\ 0 & l_{42} & l_{43} & l_{44} \end{bmatrix} \begin{Bmatrix} u_{1n}^0 \\ u_{2n}^0 \\ u_{3n}^0 \\ D_{3n}^0 \end{Bmatrix} = \omega^2 \begin{bmatrix} I_{10} & 0 & 0 & 0 \\ 0 & I_{10} & -\tilde{n}I_{11} & 0 \\ 0 & -\tilde{n}I_{11} & \left(I_{20}+\tilde{n}^2I_{12}\right) & 0 \\ 0 & 0 & 0 & 0 \end{bmatrix} \begin{Bmatrix} u_{1n}^0 \\ u_{2n}^0 \\ u_{3n}^0 \\ D_{3n}^0 \end{Bmatrix}, \tag{6.29}$$

where k_{ij} are given in (6.5) and

$$l_{24} = -\tilde{n}\tilde{F}_{32}, \quad l_{34} = \tilde{n}^2\tilde{H}_{32}+\tilde{F}_{32}, \quad l_{42} = \tilde{n}\overline{F}_{32}, \quad l_{43} = -\tilde{n}^2\overline{H}_{32}-\overline{F}_{32}, \quad l_{44} = -E_0.$$

The normal electric displacement D_{3n}^0 can be determined from the fourth equation in (6.29) and is given by

$$D_{3n}^0 = -\frac{\left(l_{42}u_{2n}^0+l_{43}u_{3n}^0\right)}{l_{44}}. \tag{6.30}$$

According to (6.30), we can rewrite (6.29) in the form

$$\begin{bmatrix} \overline{k}_{11} & 0 & 0 \\ 0 & \overline{k}_{22} & \overline{k}_{23} \\ 0 & \overline{k}_{32} & \overline{k}_{33} \end{bmatrix} \begin{Bmatrix} u_{1n}^0 \\ u_{2n}^0 \\ u_{3n}^0 \end{Bmatrix} = \omega^2 \begin{bmatrix} I_{10} & 0 & 0 \\ 0 & I_{10} & -\tilde{n}I_{11} \\ 0 & -\tilde{n}I_{11} & \left(I_{20}+\tilde{n}^2I_{12}\right) \end{bmatrix} \begin{Bmatrix} u_{1n}^0 \\ u_{2n}^0 \\ u_{3n}^0 \end{Bmatrix}, \tag{6.31}$$

where $\overline{k}_{11} = k_{11}$, $\overline{k}_{22} = k_{22}-\frac{l_{24}l_{42}}{l_{44}}$, $\overline{k}_{23} = k_{23}-\frac{l_{24}l_{43}}{l_{44}}$, $\overline{k}_{32} = k_{32}-\frac{l_{34}l_{42}}{l_{44}}$, $\overline{k}_{33} = k_{33}-\frac{l_{34}l_{43}}{l_{44}}$. The natural frequencies of the leading order for fixed n can be obtained from

$$\begin{vmatrix} \overline{k}_{11}-\omega^2I_{10} & 0 & 0 \\ 0 & \overline{k}_{22}-\omega^2I_{10} & \overline{k}_{23}+\omega^2\tilde{n}I_{11} \\ 0 & \overline{k}_{32}+\omega^2\tilde{n}I_{11} & \overline{k}_{33}-\omega^2\left(I_{20}+\tilde{n}^2I_{12}\right) \end{vmatrix} = 0. \tag{6.32}$$

At the $\in^0$-order level, the normalized eigenvectors corresponding to ω_i ($i = 1, 2, 3$) for fixed n are written as $\left\{\left(u_{1n}^0\right)_i \quad \left(u_{2n}^0\right)_i \quad \left(u_{3n}^0\right)_i\right\}^T$. Once they have been determined, the corresponding modal variables of elastic and electric fields at the leading-order level can be calculated as before.

Carrying on the solution to ϵ^2-order, we find that the nonhomogeneous terms for fixed n are

$$g_{21}(x_2, 1) = \left(\hat{g}_{21}(1)\frac{\partial \vartheta_i}{\partial t_1} + \tilde{g}_{21}(1)\right)\cos \tilde{n}x_2 \cos(\omega_i t_0 - \vartheta_i), \tag{6.33}$$

$$g_{31}(x_2, 1) = \left(\hat{g}_{31}(1)\frac{\partial \vartheta_i}{\partial t_1} + \tilde{g}_{31}(1)\right)\sin \tilde{n}x_2 \cos(\omega_i t_0 - \vartheta_i), \tag{6.34}$$

$$g_{41}(x_2, 1) = \left(\hat{g}_{41}(1)\frac{\partial \vartheta_i}{\partial t_1} + \tilde{g}_{41}(1)\right)\sin \tilde{n}x_2 \cos(\omega_i t_0 - \vartheta_i), \tag{6.35}$$

where $\hat{g}_{j1}$ and $\tilde{g}_{j1}$ $(j = 2, 3, 4)$ are the relevant coefficients.

In view of the recurrence of the equations, the ϵ^2-order solution can be obtained by letting u^1_{1n}, u^1_{2n} and u^1_{3n} be of the same form as (6.16)–(6.18) and

$$D^1_3 = D^1_{3n} \sin \tilde{n}x_2 \cos(\omega_i t_0 - \vartheta_i). \tag{6.36}$$

Substituting (6.16)–(6.18) and (6.36) in (5.33)–(5.36) gives

$$\begin{bmatrix} k_{11} - I_{10}\omega_i^2 & 0 & 0 & 0 \\ 0 & k_{22} - I_{10}\omega_i^2 & k_{23} + \tilde{n}I_{11}\omega_i^2 & l_{24} \\ 0 & k_{32} + \tilde{n}I_{11}\omega_i^2 & k_{33} - \left(I_{20} + \tilde{n}^2 I_{12}\right)\omega_i^2 & l_{34} \\ 0 & l_{42} & l_{43} & l_{44} \end{bmatrix} \begin{Bmatrix} u^1_{1n} \\ u^1_{2n} \\ u^1_{3n} \\ D^1_{3n} \end{Bmatrix}$$

$$= \begin{Bmatrix} 0 \\ \hat{g}_{21}(1)\dfrac{\partial \vartheta_{\mathrm{i}}}{\partial t_1} + \tilde{g}_{21}(1) \\ \left[\hat{g}_{31}(1) - \tilde{n}\hat{g}_{21}(1)\right]\dfrac{\partial \vartheta_{\mathrm{i}}}{\partial t_1} + \left[\tilde{g}_{31}(1) - \tilde{n}\tilde{g}_{21}(1)\right] \\ \tilde{g}_{41}(1) \end{Bmatrix}. \tag{6.37}$$

Following a solution procedure similar to that of the leading-order level, we obtain

$$D^1_{3n} = \frac{\tilde{g}_{41}(1)}{l_{44}} - \frac{I_{42}u^1_{2n}}{l_{44}} - \frac{I_{43}u^1_{3n}}{l_{44}}, \tag{6.38}$$

Equation (6.37) can then be rewritten as

$$\begin{bmatrix} \bar{k}_{11} - I_{10}\omega_i^2 & 0 & 0 \\ 0 & \bar{k}_{22} - I_{10}\omega_i^2 & \bar{k}_{23} + \tilde{n}I_{11}\omega_i^2 \\ 0 & \bar{k}_{32} + \tilde{n}I_{11}\omega_i^2 & \bar{k}_{33} - \left(I_{20} + \tilde{n}^2 I_{12}\right)\omega_i^2 \end{bmatrix} \begin{Bmatrix} u^1_{1n} \\ u^1_{2n} \\ u^1_{3n} \end{Bmatrix}$$

$$= \begin{Bmatrix} 0 \\ \hat{g}_{21}(1)\dfrac{\partial \vartheta_i}{\partial t_1} + \tilde{q}_{21}(1) \\ \left[\hat{g}_{31}(1) - \tilde{n}\hat{g}_{21}(1)\right]\dfrac{\partial \vartheta_i}{\partial t_1} + \left[\tilde{q}_{31}(1) - \tilde{n}\tilde{g}_{21}(1)\right] \end{Bmatrix}, \tag{6.39}$$

where $\tilde{q}_{21}(1) = \tilde{g}_{21}(1) - \frac{l_{24}\tilde{g}_{41}(1)}{l_{44}}$ and $\tilde{q}_{31} = \tilde{g}_{31}(1) - \frac{l_{34}\tilde{g}_{41}(1)}{l_{44}}$. The solvability condition for (6.39) is given by

$$\left(u^0_{2n}\right)_i \left\{\hat{g}_{21}(1)\frac{\partial \vartheta_{\mathrm{i}}}{\partial t_1} + \tilde{q}_{21}(1)\right\} + \left(u^0_{3n}\right)_i \left\{\left[\hat{g}_{31}(1) - \tilde{n}\hat{g}_{21}(1)\right]\frac{\partial \vartheta_{\mathrm{i}}}{\partial t_1} + \left[\tilde{q}_{31}(1) - \tilde{n}\tilde{g}_{21}(1)\right]\right\} = 0. \tag{6.40}$$

Equation (6.39) is solvable if and only if the solvability condition (6.40) is satisfied. Collecting the terms of $\partial \vartheta_i / \partial t_1$, we may rewrite Eq. (6.40) in the form

$$\left\{\left(u^0_{2n}\right)_i \hat{g}_{21}(1) + \left(u^0_{3n}\right)_i \left[\hat{g}_{31}(1) - \tilde{n}\hat{g}_{21}(1)\right]\right\}\frac{\partial \vartheta_i}{\partial t_1} + \left\{\left(u^0_{2n}\right)_i \tilde{q}_{21}(1) + \left(u^0_{3n}\right)_i \left[\tilde{q}_{31}(1) - \tilde{n}\tilde{g}_{21}(1)\right]\right\} = 0. \tag{6.41}$$

Since the coefficients of $(\partial\vartheta_i/\partial t_1)$ in (6.41) are constants, The dependence of ϑ_i, upon t_1 can be determined as

$$\vartheta_i = -\lambda_i t_1 + \overline{\vartheta}_i(t_2, t_3, \ldots), \tag{6.42}$$

where $\lambda_i = \frac{(u^0_{2n})_i \tilde{q}_{21}(1) + (u^0_{3n})_i [\tilde{q}_{31}(1) - \tilde{n}\tilde{g}_{21}(1)]}{(u^0_{2n})_i \hat{g}_{21}(1) + (u^0_{3n})_i [\hat{g}_{31}(1) - \tilde{n}\hat{g}_{21}(1)]}$.

With (6.42) and the relation $t_1 = \epsilon^2 t_0 = (h/R)t_0$, the time functions of all field variables are now expressed in terms of $\cos\left[(\omega + \lambda h/R)\, t_0 - \overline{\vartheta}\right]$. Therefore, the natural frequencies at the ϵ^2-order level have been modified to $\omega_i + \lambda_i \frac{h}{R}$ $(i = 1, 2, 3)$.

Substituting (6.42) into (6.39) yields

$$\begin{bmatrix} \overline{k}_{11} - I_{10}\omega_i^2 & 0 & 0 \\ 0 & \overline{k}_{22} - I_{10}\omega_i^2 & \overline{k}_{23} + \tilde{n} I_{11}\omega_i^2 \\ 0 & \overline{k}_{32} + \tilde{n} I_{11}\omega_i^2 & \overline{k}_{33} - \left(I_{20} + \tilde{n}^2 I_{12}\right)\omega_i^2 \end{bmatrix} \begin{Bmatrix} u^1_{1n} \\ u^1_{2n} \\ u^1_{3n} \end{Bmatrix}$$
$$= \begin{Bmatrix} 0 \\ -\lambda_i \hat{g}_{21}(1) + \tilde{q}_{21}(1) \\ -\lambda_i \left[\hat{g}_{31}(1) - \tilde{n}\hat{g}_{21}(1)\right] + \left[\tilde{q}_{31}(1) - \tilde{n}\tilde{g}_{21}(1)\right] \end{Bmatrix}. \tag{6.43}$$

The variables of u^1_{1n}, u^1_{2n} and u^1_{3n} can be determined from (6.43) and the modifications of the other modal variables of the ϵ^2-order are subsequently determined as before. The solution process can be repeatedly applied for various order problems and the asymptotic solutions can be obtained hierarchically.

7 Illustrative examples

The cylindrical bending vibrations of multilayered and FG piezoelectric cylindrical shells are considered using the present asymptotic formulations. The material properties of those shells are described as follows:

Type 1—multilayered piezoelectric cylindrical shells.
The cylindrical bending vibration of multilayered piezoelectric shells can be regarded as a special case of the present subject where the material-property variations of the shells through the thickness coordinate are layerwise Heaviside functions and are given by

$$m_{ij}(\zeta) = \sum_{k=1}^{NL} m_{ij}^{(k)} \left[H(\zeta - \zeta_k) - H(\zeta - \zeta_{k+1})\right], \tag{7.1}$$

where m_{ij} refer to material coefficients of c_{ij}, e_{ij} and η_{ij}; $H(\zeta)$ is the Heaviside function and ζ_k is the distance measured from the middle surface of the shell to the bottom surface of the kth layer.

Type 2—functionally graded piezoelectric shells.
For a Type 2 shell, the material properties are assumed to obey the identical exponent law varied exponentially with the thickness coordinate and are given by

$$m_{ij} = m_{ij}^{(b)} \mathrm{e}^{\alpha[(\zeta + h)/2h]}, \tag{7.2}$$

where the superscript b in parentheses denotes the bottom surface; α is the material-property gradient index which represents the degree of the material gradient along the thickness.

7.1 Multilayered piezoelectric plates

The available exact solutions of cylindrical bending vibration problems of $[A/B]$ two-layered piezoelectric plates [5] are used to validate the present asymptotic formulations where the total thickness and the in-plane dimension

are $2h$ and L. By letting $1/R = 0$ and $a_\theta = L$, we may reduce the present asymptotic formulations of piezoelectric cylindrical shells to those of piezoelectric plates. For comparison purposes, the geometric parameters of the two-layered plates and the material properties of each layer are identical to those given in the literature [5]. Both layers are of equal thickness and the total thickness is taken as 0.01 m. The elastic, piezoelectric and dielectric properties of piezoceramic materials A and B are given in Table 1. Table 2 shows the present asymptotic results of fundamental frequencies for $[A/B]$ two-layered piezoelectric plates with either open-circuit or closed-circuit surface conditions where the values of $a_\theta/2h$ are taken as 4, 10, 50 and 100. It is shown that the present asymptotic solutions converge rapidly. The convergent solutions yield at the ϵ^6-order level in the cases of thick plates ($a_\theta/2h = 4$), at the ϵ^4-order level in the cases of moderately thick plates ($a_\theta/2h = 10$) and at the ϵ^2-order level in the cases of thin plates ($a_\theta/2h = 100$). The present convergent solutions are observed from Table 2 to be in excellent agreement with the available exact solutions [5]. The non-piezoelectricity results given in parentheses are obtained by letting $e_{ij} = 0$. The effect of piezoelectricity on the fundamental frequencies of two-layered piezoelectric plates is also examined. It is shown that the fundamental frequencies of piezoelectric plates are higher than those of non-pioezoelectric plates. The effect of piezoelectricity does make the plates stiffer. In addition, the fundamental frequencies of piezoelectric plates with open-circuit surface conditions are slightly larger than those of piezoelectric plates with closed-circuit surface conditions. The deviation for the fundamental frequencies of plates with open-circuit and closed-circuit surface conditions decreases, as the plate becomes thinner.

Table 3 shows the natural frequencies of $[A/B]$ two-layered piezoelectric plates with two different surface conditions where the wave number n is taken as 1, 2, 3, 4, 5 and $a_\theta/2h = 10$. Again, the present asymptotic solutions are shown to converge rapidly and to be in good agreement with the solutions obtained from a 2D accurate theory by Shu [4]. The natural frequencies of piezoelectric plates with open-circuit surface conditions are slightly larger than those of piezoelectric plates with closed-circuit surface conditions for various vibration modes. The deviation for the fundamental frequencies of the plates with open-circuit and closed-circuit surface conditions increases, as the wave number n becomes larger.

Table 1 Elastic, piezoelectric and dielectric properties of piezoelectric materials

	Material A [5]	Material B [5]		PZT-4 [25]
E_1 (GPa)	81.3	136.0	c_{11} (GPa)	139.0
E_2	81.3	136.0	c_{22}	139.0
E_3	64.5	116.0	c_{33}	115.0
υ_{12}	0.329	0.204	c_{12}	77.8
υ_{13}	0.432	0.201	c_{13}	74.3
υ_{23}	0.432	0.201	c_{23}	74.3
G_{23}	25.6	55.2	c_{44}	25.6
G_{13}	25.6	55.2	c_{55}	25.6
G_{12}	30.6	56.5	c_{66}	30.6
e_{31} $(\mathrm{C/m^2})$	−5.20	−5.35	e_{31} $(\mathrm{C/m^2})$	−5.2
e_{32}	−5.20	−5.35	e_{32}	−5.2
e_{33}	15.08	15.78	e_{33}	15.1
e_{24}	12.72	12.29	e_{24}	12.7
e_{15}	12.72	12.29	e_{15}	12.7
η_{11}/ε_0	1,475	1,730	η_{11} $(\mathrm{C^2/Nm^2})$	6.46×10^{-9}
η_{22}/ε_0	1,475	1,730	η_{22}	6.46×10^{-9}
η_{33}/ε_0	1,300	1,700	η_{33}	5.62×10^{-9}
ρ/ρ_0	1.0	1.0	ρ $(\mathrm{kg/m^3})$	7,600

$\varepsilon_0 = 8.854 \times 10^{-12}$ F/m

Table 2 Fundamental frequencies ω for the flexural modes of two-layered piezoelectric plates ($n = 1$)

Surface conditions	$a_\theta/2h$	Present solutions					3D exact solution
		ϵ^0	ϵ^2	ϵ^4	ϵ^6	ϵ^8	[5]
Open	4	0.6139×10^7 (0.5817×10^7)	0.5694×10^7 (0.5347×10^7)	0.5742×10^7 (0.5402×10^7)	0.5737×10^7 (0.5396×10^7)	0.5737×10^7 (0.5396×10^7)	0.5706×10^7 (NA)
	10	1.0033×10^6 (0.9511×10^6)	0.9907×10^6 (0.9377×10^6)	0.9909×10^6 (0.9380×10^6)	0.9909×10^6 (0.9380×10^6)	0.9909×10^6 (0.9380×10^6)	NA (NA)
	50	0.4030×10^5 (0.3820×10^5)	0.4028×10^5 (0.3818×10^5)	0.4028×10^5 (0.3818×10^5)	0.4028×10^5 (0.3818×10^5)	0.4028×10^5 (0.3818×10^5)	0.3995×10^5 (NA)
	100	1.0075×10^4 (0.9551×10^4)	1.0074×10^4 (0.9550×10^4)	1.0074×10^4 (0.9550×10^4)	1.0074×10^4 (0.9550×10^4)	1.0074×10^4 (0.9550×10^4)	NA (NA)
Closed	4	0.6087×10^7 (0.5817×10^7)	0.5620×10^7 (0.5347×10^7)	0.5674×10^7 (0.5402×10^7)	0.5667×10^7 (0.5395×10^7)	0.5668×10^7 (0.5396×10^7)	0.5649×10^7 (NA)
	10	0.9951×10^6 (0.9511×10^6)	0.9817×10^6 (0.9377×10^6)	0.9820×10^6 (0.9380×10^6)	0.9820×10^6 (0.9380×10^6)	0.9820×10^6 (0.9380×10^6)	NA (NA)
	50	0.3997×10^5 (0.3820×10^5)	0.3995×10^5 (0.3818×10^5)	0.3995×10^5 (0.3818×10^5)	0.3995×10^5 (0.3818×10^5)	0.3995×10^5 (0.3818×10^5)	0.3981×10^5 (NA)
	100	0.9993×10^4 (0.9551×10^4)	0.9992×10^4 (0.9550×10^4)	0.9992×10^4 (0.9550×10^4)	0.9992×10^4 (0.9550×10^4)	0.9992×10^4 (0.9550×10^4)	NA (NA)

Table 3 Natural frequencies ω for the flexural modes of two-layered piezoelectric plates ($a_\theta/2h = 10$)

Surface conditions	n	Present solutions					2D accurate theory
		ϵ^0	ϵ^2	ϵ^4	ϵ^6	ϵ^8	[4]
Open	1	1.0033×10^6 (0.9511×10^6)	0.9907×10^6 (0.9377×10^6)	0.9909×10^6 (0.9380×10^6)	0.9909×10^6 (0.9380×10^6)	0.9909×10^6 (0.9380×10^6)	NA (NA)
	2	0.3964×10^7 (0.3757×10^7)	0.3774×10^7 (0.3555×10^7)	0.3788×10^7 (0.3571×10^7)	0.3787×10^7 (0.3570×10^7)	0.3787×10^7 (0.3570×10^7)	NA (NA)
	3	0.8744×10^7 (0.8284×10^7)	0.7873×10^7 (0.7365×10^7)	0.7998×10^7 (0.7506×10^7)	0.7980×10^7 (0.7487×10^7)	0.7982×10^7 (0.7489×10^7)	NA (NA)
	4	0.1514×10^8 (0.1433×10^8)	0.1274×10^8 (0.1182×10^8)	0.1324×10^8 (0.1237×10^8)	0.1315×10^8 (0.1228×10^8)	0.1316×10^8 (0.1228×10^8)	NA (NA)
	5	0.2290×10^8 (0.2167×10^8)	0.1795×10^8 (0.1651×10^8)	0.1919×10^8 (0.1782×10^8)	0.1902×10^8 (0.1774×10^8)	0.1896×10^8 (0.1757×10^8)	NA (NA)
Closed	1	0.9951×10^6 (0.9511×10^6)	0.9817×10^6 (0.9377×10^6)	0.9820×10^6 (0.9380×10^6)	0.9820×10^6 (0.9380×10^6)	0.9820×10^6 (0.9380×10^6)	0.9848×10^6 (0.9372×10^6)
	2	0.3931×10^7 (0.3757×10^7)	0.3730×10^7 (0.3555×10^7)	0.3746×10^7 (0.3571×10^7)	0.3745×10^7 (0.3570×10^7)	0.3745×10^7 (0.3570×10^7)	0.3733×10^7 (0.3559×10^7)
	3	0.8669×10^7 (0.8284×10^7)	0.7759×10^7 (0.7365×10^7)	0.7895×10^7 (0.7506×10^7)	0.7876×10^7 (0.7486×10^7)	0.7878×10^7 (0.7488×10^7)	0.7789×10^7 (0.7445×10^7)
	4	0.1500×10^8 (0.1433×10^8)	0.1252×10^8 (0.1182×10^8)	0.1304×10^8 (0.1236×10^8)	0.1296×10^8 (0.1228×10^8)	0.1296×10^8 (0.1227×10^8)	0.1271×10^8 (0.1218×10^8)
	5	0.2269×10^8 (0.2167×10^8)	0.1764×10^8 (0.1651×10^8)	0.1883×10^8 (0.1780×10^8)	0.1880×10^8 (0.1773×10^8)	0.1862×10^8 (0.1755×10^8)	0.1817×10^8 (0.1745×10^8)

7.2 Functionally graded piezoelectric cylindrical shells

The cylindrical bending vibration of FG piezoelectric cylindrical shells with two different surface conditions is considered in Table 4 and Figs. 2, 3. The material properties are assumed to obey the identical exponent law varied exponentially with the thickness coordinate and are given in (7.2). The material properties of PZT-4 [25] are used as the reference material properties (Table 1) and placed at the bottom surface (i.e., $c_{ij}^{(b)}$, $e_{ij}^{(b)}$, $\eta_{ij}^{(b)}$ where the superscript b in parentheses denotes the bottom surface.). The ratio of material properties between top and bottom surfaces is given as

$$\frac{c_{ij}^{(t)}}{c_{ij}^{(b)}} = \frac{e_{ij}^{(t)}}{e_{ij}^{(b)}} = \frac{\eta_{ij}^{(t)}}{\eta_{ij}^{(b)}} = \mathrm{e}^{\alpha}, \tag{7.3}$$

where the superscript t in parentheses denotes the top surface. In the case of $\alpha = 0$, the FG piezoelectric shells will reduce to single-layer homogeneous piezoelectric shells with the material properties of the bottom surface.

Table 4 shows the fundamental frequencies of FG piezoelectric shells with two different surface conditions. The geometric parameters of the piezoelectric shells are taken as $R/a_\theta = 1, 5, 1{,}0000$; $2h/a_\theta = 0.1, 0.2$. The material-property index is taken as $\alpha = 1.0$ and 3.0. It is shown that the fundamental frequencies of FG piezoelectric shells increses as the values of R/a_θ and $2h/a_\theta$ become larger and as the value of α becomes smaller.

Table 4 Fundamental frequency parameters Ω for FG piezoelectric shells $\left(\Omega = 2h\omega\sqrt{\rho^{(b)}/c_{11}^{(b)}}/2\pi,\ n = 1\right)$

Surface conditions	α	$2h/a_\theta$	R/a_θ	Present solutions				
				ϵ^0	ϵ^2	ϵ^4	ϵ^6	ϵ^8
Open	1	0.1	1	0.00390	0.00344	0.00345	0.00345	0.00345
			5	0.00409	0.00402	0.00402	0.00402	0.00402
			10,000	0.00410	0.00405	0.00405	0.00405	0.00405
Closed	1	0.1	1	0.00385	0.00338	0.00339	0.00339	0.00339
			5	0.00404	0.00396	0.00396	0.00396	0.00396
			10,000	0.00405	0.00399	0.00399	0.00399	0.00399
Open	1	0.2	1	0.01546	0.01305	0.01317	0.01317	0.01317
			5	0.01617	0.01534	0.01539	0.01539	0.01539
			10,000	0.01622	0.01549	0.01554	0.01554	0.01554
Closed	1	0.2	1	0.01524	0.01271	0.01287	0.01287	0.01287
			5	0.01596	0.01499	0.01506	0.01506	0.01506
			10,000	0.01601	0.01514	0.01522	0.01521	0.01521
Open	3	0.1	1	0.00326	0.00283	0.00284	0.00284	0.00284
			5	0.00344	0.00337	0.00337	0.00337	0.00337
			10,000	0.00345	0.00341	0.00341	0.00341	0.00341
Closed	3	0.1	1	0.00305	0.00266	0.00267	0.00267	0.00267
			5	0.00322	0.00316	0.00316	0.00316	0.00316
			10,000	0.00324	0.00320	0.00320	0.00320	0.00320
Open	3	0.2	1	0.01286	0.01051	0.01069	0.01068	0.01068
			5	0.01361	0.01279	0.01286	0.01285	0.01285
			10,000	0.01368	0.01302	0.01307	0.01307	0.01307
Closed	3	0.2	1	0.01203	0.00985	0.01003	0.01002	0.01002
			5	0.01276	0.01199	0.01205	0.01205	0.01205
			10,000	0.01285	0.01221	0.01226	0.01226	0.01226

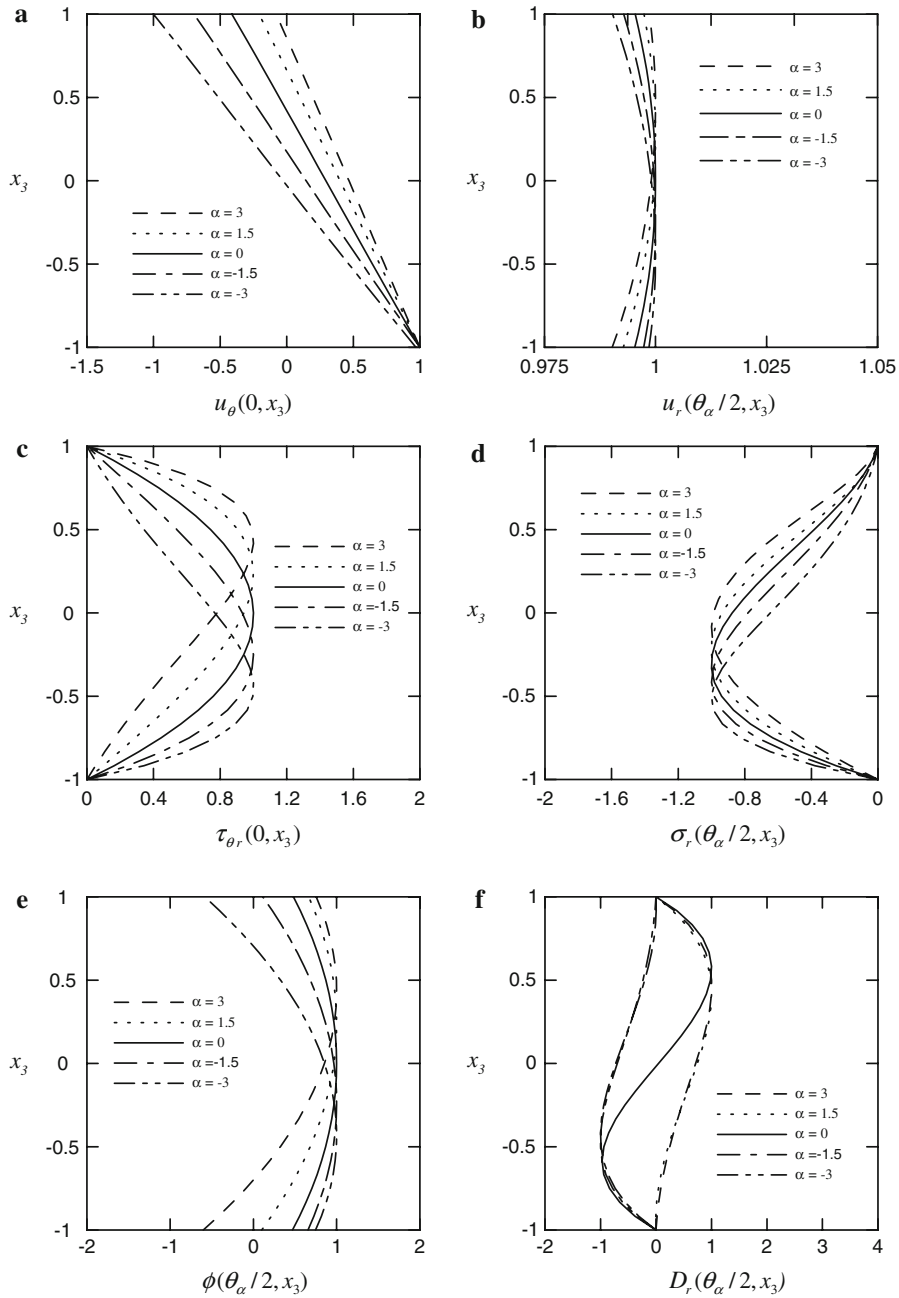

Fig. 2 The through-thickness distributions of the modal field variables in the FG piezoelectric shells with open-circuit surface conditions and different values of the material-property gradient index

Figures 2, 3 show the distributions for modal variables of mechanical and electric fields across the thickness coordinate for the fundamental vibration mode of a FG shell with open-circuit and closed-circuit surface conditions, respectively. The material-property index is taken as $\alpha = -3.0, -1.5, 0, 1.5, 3.0$. The geometric parameters are $2h/a_\theta = 0.1$ and $R/a_\theta = 5$. It is observed from Figs. 3, 4 that the through-thickness distributions of mechanical field variables for plates with open-circuit surface conditions reveal similar patterns as those for plates with closed-circuit surface conditions. However, the through-thickness distributions of electric-field variables for plates with open-circuit surface conditions reveal different patterns as those for plates with closed-circuit surface conditions.

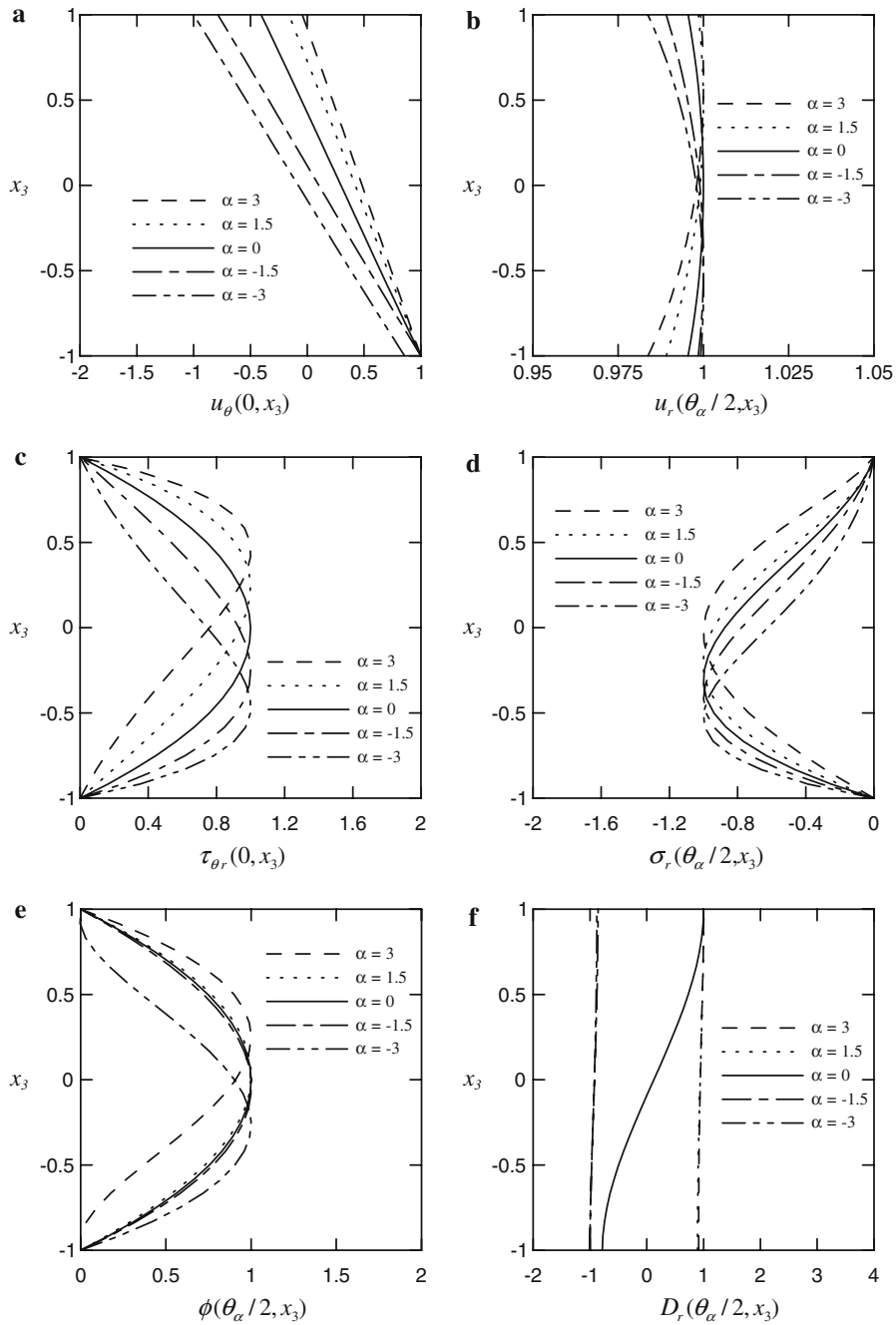

Fig. 3 The through-thickness distributions of the modal field variables in the FG piezoelectric shells with closed-circuit surface conditions and different values of material-property gradient index

8 Concluding remarks

Based on the method of multiple time scales, we have developed two asymptotic formulations for the cylindrical bending vibration of FG piezoelectric shells with open-circuit and closed-circuit surface conditions, respectively.

Through a straightforward manipulation, such as nondimensionalization, asymptotic expansions, successive integration etc, we obtained two recursive sets of CST-type equations of motion for various order problems. In the cases of open-circuit conditions, the variables of the electric potential and elastic displacements are the generalized kinematics field variables in the equations of motion for various order problems; whereas the variables of the normal electric displacement and elastic displacements become so for closed-circuit conditions. These formulations have been shown to be feasible in a systematic manner. Applications of the present formulations to illustrative examples show that the present asymptotic solutions converge rapidly and are in excellent agreement with exact solutions available in the literature. It is noted that the natural frequencies of shells with open-circuit surface conditions are slightly higher than those of shells with closed-circuit surface conditions. The through-thickness distributions of the modal elastic variables reveal similar patterns for the two surface conditions; however, different patterns of those distributions are observed for the modal electric variables.

Acknowledgements This work is supported by the National Science Council of Republic of China through Grant NSC 96-2221-E006-265.

A Appendix

A.1 Shells with open-circuit surface conditions ($j = 0$)

The relevant functions of φ_{ik} and f_{ik} ($i = 2$–4, $k = 1, 2, 3, \ldots$) in Eqs. (5.13)–(5.20) are given by

$$\varphi_{2k}(x_2, x_3) = -x_3 u_2^{(k-1)} + \int_0^{x_3} \left[2u_2^{(k-1)} + \tilde{s}_{44}\tau_{23}^{(k-1)} + (x_3\tilde{s}_{44})\tau_{23}^{(k-2)} - \varphi_{3k,2} - (\tilde{s}_{44}\tilde{e}_{24})\varphi_{4k,2} \right] \mathrm{d}\eta,$$

$$\varphi_{3k}(x_2, x_3) = -\int_0^{x_3} \left[\bar{a}_2 u_2^{(k-1)}{}_{,2} + \bar{a}_2 u_3^{(k-1)} - \tilde{e} D_3^{(k-1)} - \tilde{\eta}\sigma_3^{(k-2)} \right] \mathrm{d}\eta,$$

$$\varphi_{4k}(x_2, x_3) = -\int_0^{x_3} \left[\bar{b}_2 u_2^{(k-1)}{}_{,2} + \bar{b}_2 u_3^{(k-1)} + \tilde{c} D_3^{(k-1)} - \tilde{e}\sigma_3^{(k-2)} \right] \mathrm{d}\eta,$$

$$\begin{aligned} f_{2k}(x_2, x_3) = {} & x_3\tau_{23}^{(k-1)} + \int_{-1}^{x_3} \left[\overline{Q}_{22}\varphi_{2k,22} + \overline{Q}_{22}\varphi_{3k,2} + \tilde{b}_2 f_{4k,2} + \tau_{23}^{(k-1)} + \tilde{a}_2\sigma_3^{(k-1)}{}_{,2} \right] \mathrm{d}\eta \\ & - \left[\frac{\partial^2}{\partial t_0^2} \left(\int_{-1}^{x_3} \rho_1\varphi_{2k}\mathrm{d}\eta \right) + \frac{\partial^2}{\partial t_0 \partial t_1} \left(\int_{-1}^{x_3} 2\rho_1 u_2^{(k-1)}\mathrm{d}\eta \right) + \cdots + \left(\frac{\partial^2}{\partial t_0 \partial t_k} + \frac{\partial^2}{\partial t_1 \partial t_{k-1}} \right. \right. \\ & \left. \left. + \cdots + \frac{\partial^2}{\partial t_k \partial t_0} \right) \left(\int_{-1}^{x_3} \rho_1 u_2^{(0)}\mathrm{d}\eta \right) \right], \end{aligned}$$

$$\begin{aligned} f_{3k}(x_2, x_3) = {} & x_3\sigma_3^{(k-1)} - \int_{-1}^{x_3} \left[\overline{Q}_{22}\varphi_{2k,2} + \overline{Q}_{22}\varphi_{3k} - \tilde{b}_2 f_{4k} + f_{2k,2} + \tilde{a}_2\sigma_3^{(k-1)} \right] \mathrm{d}\eta \\ & - \left[\frac{\partial^2}{\partial t_0^2} \left(\int_{-1}^{x_3} \rho_2\varphi_{3k}\mathrm{d}\eta \right) + \frac{\partial^2}{\partial t_0 \partial t_1} \left(\int_{-1}^{x_3} 2\rho_2 u_3^{(k-1)}\mathrm{d}\eta \right) + \cdots \right. \\ & \left. + \left(\frac{\partial^2}{\partial t_0 \partial t_k} + \frac{\partial^2}{\partial t_1 \partial t_{k-1}} + \cdots + \frac{\partial^2}{\partial t_k \partial t_0} \right) \left(\int_{-1}^{x_3} \rho_2 u_3^{(0)}\mathrm{d}\eta \right) \right], \end{aligned}$$

$$f_{4k}(x_2, x_3) = x_3 D_3^{(k-1)} + \int_{-1}^{x_3} \left[(\tilde{s}_{44}\tilde{e}_{24})\tau_{23}^{(k-1)}{}_{,2} - (1/\gamma_\theta) \left(\tilde{s}_{44}\tilde{e}_{24} + \frac{\eta_{22} Q}{e^2} \right) \varphi_{4k,22} \right] \mathrm{d}\eta.$$

A.2 Shells with closed-circuit surface conditions ($j = 2$)

The relevant functions of ψ_{ik} and g_{ik} ($i = 2$–4, $k = 1, 2, 3, \ldots$) in Eqs. (5.29)–(5.36) are

$$\psi_{2k}(x_2, x_3) = -x_3 u_2^{(k-1)} + \int_0^{x_3} \left[2u_2^{(k-1)} + \tilde{s}_{44}\tau_{23}^{(k-1)} + (x_3\tilde{s}_{44})\tau_{23}^{(k-2)} - \psi_{3k,2} - (\tilde{s}_{44}\tilde{e}_{24})\psi_{4k,2} \right] \mathrm{d}\eta,$$

$$\psi_{3k}(x_2, x_3) = -\int_0^{x_3} \left[\overline{a}_2 u_2^{(k-1)}{}_{,2} + \overline{a}_2 u_3^{(k-1)} - \tilde{e} D_3^{(k-1)} - \tilde{\eta}\sigma_3^{(k-2)} \right] \mathrm{d}\eta,$$

$$\psi_{4k} = x_3 D_3^{(k-1)} - \int_0^{x_3} \left[\tilde{s}_{44}\tilde{e}_{44}\tau_{23}^{(k-1)}{}_{,2} - \left(\tilde{s}_{44}\tilde{e}_{24}^2 + \frac{\eta_{22} Q}{e^2} \right) (1/\gamma_\theta)\phi^{(k-1)}{}_{,22} \right] \mathrm{d}\eta,$$

$$\begin{aligned} g_{2k}(x_2, x_3) = {} & x_3\tau_{23}^{(k-1)} + \int_{-1}^{x_3} \left[\overline{Q}_{22}\psi_{2k,22} + \overline{Q}_{22}\psi_{3k,2} - \tilde{b}_2 f_{4k\cdot 2} + \tau_{23}^{(k-1)} + \tilde{a}_2\sigma_3^{(k-1)}{}_{,2} \right] \mathrm{d}\eta \\ & - \left[\frac{\partial^2}{\partial t_0^2} \left(\int_{-1}^{x_3} \rho_1\psi_{2k}\mathrm{d}\eta \right) + \frac{\partial^2}{\partial t_0 \partial t_1} \left(\int_{-1}^{x_3} 2\rho_1 u_2^{(k-1)}\mathrm{d}\eta \right) + \cdots \right. \\ & \left. + \left(\frac{\partial^2}{\partial t_0 \partial t_k} + \frac{\partial^2}{\partial t_1 \partial t_{k-1}} + \cdots + \frac{\partial^2}{\partial t_k \partial t_0} \right) \left(\int_{-1}^{x_3} \rho_1 u_2^{(0)}\mathrm{d}\eta \right) \right], \end{aligned}$$

$$\begin{aligned} g_{3k}(x_2, x_3) = {} & x_3\sigma_3^{(k-1)} - \int_{-1}^{x_3} \left[\overline{Q}_{22}\psi_{2k,2} + \overline{Q}_{22}\psi_{3k} - \tilde{b}_2 D_3^{(k)} + f_{2k,2} + \tilde{a}_2\sigma_3^{(k-1)} \right] \mathrm{d}\eta \\ & - \left[\frac{\partial^2}{\partial t_0^2} \left(\int_{-1}^{x_3} \rho_2\psi_{3k}\mathrm{d}\eta \right) + \frac{\partial^2}{\partial t_0 \partial t_1} \left(\int_{-1}^{x_3} 2\rho_2 u_3^{(k-1)}\mathrm{d}\eta \right) + \cdots \right. \\ & \left. + \left(\frac{\partial^2}{\partial t_0 \partial t_k} + \frac{\partial^2}{\partial t_1 \partial t_{k-1}} + \cdots + \frac{\partial^2}{\partial t_k \partial t_0} \right) \left(\int_{-1}^{x_3} \rho_2 u_3^{(0)}\mathrm{d}\eta \right) \right], \end{aligned}$$

$$g_{4k}(x_2, x_3) = \int_{-1}^{x_3} \left[\tilde{b}_2\psi_{2k,2} + \tilde{b}_2\psi_{3k} + \tilde{c}\psi_{4k} - \tilde{e}\sigma_3^{(k-1)} \right] \mathrm{d}\eta.$$

References

1. Hussein M, Heyliger P (1998) Three-dimensional vibrations of layered piezoelectric cylinders. J Eng Mech ASCE 124:1294–1298
2. Kharouf N, Heyliger PR (1994) Axisymmetric free vibrations of homogeneous and laminated piezoelectric cylinders. J Sound Vib 174:539–561
3. Heyliger PR, Ramirez G (2000) Free vibration of laminated circular piezoelectric plates and discs. J Sound Vib 229:935–956
4. Shu X (2005) Free vibration of laminated piezoelectric composite plates based on an accurate theory. Compos Struct 67:375–382
5. Heyliger P, Brooks S (1995) Free vibration of piezoelectric laminates in cylindrical bending. Int J Solids Struct 132:2945–2960
6. Heyliger P, Brooks S (1996) Exact solutions for laminated piezoelectric plates in cylindrical bending. J Appl Mech 63:903–910
7. Pagano NJ (1969) Exact solutions for composite laminates in cylindrical bending. J Compos Mater 3:398–411
8. Vel SS, Mewer RC, Batra RC (2004) Analytical solution for the cylindrical bending vibration of piezoelectric composite plates. Int J Solids Struct 41:1625–1643
9. Vel SS, Batra RC (2001) Exact solution for rectangular sandwich plates with embedded piezoelectric shear actuators. AIAA J 39:1363–1373
10. Lü CF, Huang ZY, Chen WQ (2007) Semi-analytical solutions for free vibration of anisotropic laminated plates in cylindrical bending. J Sound Vib 304:987–995
11. Jin J, Batra RC (2005) Effect of electromechanical coupling on static deformations and natural frequencies. IEEE Trans Ultrason Ferroelectr Freq Control 52:1079–1093
12. Tang YY, Noor AK, Xu K (1996) Assessment of computational models for thermoelectroelastic multilayered plates. Comput Struct 61:915–933
13. Saravanos SA, Heyliger PR (1999) Mechanics and computational models for laminated piezoelectric beams, plates and shells. Appl Mech Rev 52:305–319

14. Gopinathan SV, Varadan VV, Varadan VK (2000) A review and critique of theories for piezoelectric laminates. Smart Mater Struct 9:24–48
15. Chee CYK, Tong L, Steven GP (1998) A review on the modeling of piezoelectric sensors and actuators incorporated in intelligent structures. J Intell Mater Syst Struct 9:3–19
16. Ramirez F, Heyliger PR, Pan E (2006) Static analysis of functionally graded elastic anisotropic plates using a discrete layer approach. Compos Part B 27:10–20
17. Chen WQ, Ding HJ (2002) On free vibration of a functionally graded piezoelectric rectangular plate. Acta Mech 153:207–216
18. Wu CP, Liu KY (2007) A state space approach for the analysis of doubly curved functionally graded elastic and piezoelectric shells. CMC: Comp Mater Continua 6:177–199
19. Soldatos KP, Hadjigeorgiou VP (1990) Three-dimensional solution of the free vibration problem of homogeneous isotropic cylindrical shells and plates. J Sound Vib 137:369–384
20. Shuvalov AL, Soldatos KP (2003) On the successive approximation method for three-dimensional analysis of radially inhomogeneous tubes with an arbitrary cylindrical anisotropy. J Sound Vib 259:233–239
21. Shuvalov AL (2003) A sextic formalism for three-dimensional elastodynamics of cylindrically anisotropic radially inhomogeneous materials. Proc R Soc Lond A 459:1611–1639
22. Vel SS, Batra RC (2004) Three-dimensional exact solution for the vibration of functionally graded rectangular plates. J Sound Vib 272:703–730
23. Mori T, Tanaka K (1973) Average stress in matrix and average elastic energy of materials with misfitting inclusions. Acta Metallurg 21:571–574
24. Hill R (1965) A self-consistent mechanics of composite materials. J Mech Phys Solids 13:213–222
25. Zhong Z, Yu T (2006) Vibration of a simply supported functionally graded piezoelectric rectangular plate. Smart Mater Struct 15:1404–1412
26. Wang YM, Tarn JQ (1994) Three-dimensional analysis of anisotropic inhomogeneous and laminated plates. Int J Solids Struct 31:497–515
27. Tarn JQ, Wang YM (1995) Asymptotic theory for dynamic response of anisotropic inhomogeneous and laminated plates. Int J Solids Struct 31:231–246
28. Tarn JQ, Wang YM (1995) Asymptotic thermoelastic analysis of anisotropic inhomogeneous and laminated plates. J Therm Stresses 18:35–58
29. Wu CP, Tarn JQ, Chi SM (1996) Three-dimensional analysis of doubly curved laminated shells. J Eng Mech ASCE 122:391–401
30. Wu CP, Tarn JQ, Chi SM (1996) An asymptotic theory for dynamic response of doubly curved laminated shells. Int J Solids Struct 33:3813–3841
31. Wu CP, Chiu SJ (2002) Thermally induced dynamic instability of laminated composite conical shells. Int J Solids Struct 39: 3001–3021
32. Wu CP, Chi YW (2005) Three-dimensional nonlinear analysis of laminated cylindrical shells under cylindrical bending. Euro J Mech A/Solids 24:837–856
33. Cheng ZQ, Batra RC (2000) Three-dimensional asymptotic analysis of multiple-electroded piezoelectric laminates. AIAA J 38:317–324
34. Cheng ZQ, Batra RC (2000) Three-dimensional asymptotic scheme for piezothermoelastic laminates. J Therm Stresses 23:95–110
35. Wu CP, Lo JY, Chao JK (2005) A three-dimensional asymptotic theory of laminated piezoelectric shells. CMC: Comput Mater Continua 2:119–137
36. Wu CP, Lo JY (2006) An asymptotic theory for dynamic response of laminated piezoelectric shells. Acta Mech 183:177–208
37. Nayfeh AH (1981) Introduction to perturbation techniques. Wiley, 519 pp
38. Nayfeh AH, Mook DT (1979) Nonlinear oscillations. Wiley, 704 pp